SOLAR RADIATION ESTIMATION FOR MODELING OF PV ARRAYS AND CALCULATION OF SOLAR ENERGY POTENTIAL BASED ON ArcGIS

Master of Science Thesis

Kübra BİTİRGEN

Eskişehir, 2018

SOLAR RADIATION ESTIMATION FOR MODELING OF PV ARRAYS AND CALCULATION OF SOLAR ENERGY POTENTIAL BASED ON ArcGIS

Kübra BİTİRGEN

MASTER OF SCIENCE THESIS

Graduate School of Sciences
Electrical and Electronics Engineering Program
Supervisor: Assist. Prof. Dr. Ümmühan BAŞARAN FİLİK

Eskişehir
Anadolu University
Graduate School of Sciences
June, 2018

FINAL APPROVAL FOR THESIS

This thesis titled " Solar Radiation Estimation for Modeling of PV Arrays and Calculation of Solar Energy Potential Based on ArcGIS " has been prepared and submitted by Kübra BİTİRGEN in partial fullfillment of the requirements in "Anadolu University Directive on Graduate Education and Examination" for the Degree of Master of Science in Electrical and Electronics Engineering Department has been examined and approved on 05/06/2018.

Committee Members	Title Name Surname	Signature
Member(Supervisor)	: Assist. Prof.Dr. Ümmühan Başaran Filik	....
Member	: Prof.Dr. Mehmet Kurban	....
Member	: Assist. Prof.Dr. Şener Ağalar	....

Prof.Dr. Ersin YÜCEL

Director of Graduate School of Sciences

ABSTRACT

SOLAR RADIATION ESTIMATION FOR MODELING OF PV ARRAYS AND CALCULATION OF SOLAR ENERGY POTENTIAL BASED ON ArcGIS

Kübra BİTİRGEN

Electrical and Electronics Engineering Program

Anadolu University, Graduate School of Sciences, June, 2018

Supervisor: Assist. Prof. Dr. Ümmühan BAŞARAN FİLİK

Solar energy is known as one of the most efficient alternative energy resources. Solar radiation reaching to the earth is a form of the solar energy. Solar energy applications require a complete knowledge and detailed analysis on the solar radiation potential of the selected place. In this thesis, hourly global solar radiation on a sloped surface is estimated for Eskişehir by implementing six different solar radiation calculation models. The outputs of this models are compared with hourly ground measured data by using statistical error methods. The estimation results are converted to monthly global solar radiation to show the performance of the models more specifically. After selecting the available solar radiation model, when comparing the models, the model which gives more accurate results is used to calculate the PV potential of Eskişehir. An ideal photovoltaic panel (PV) simulation is implemented in MATLAB Simulink program besides that one suitable algorithm is selected to calculate the possible amount of PV panel energy generation based on the hourly measured wind speed, air pressure, global solar radiation and temperature values. After determination of PV potential, ideal PV simulation and estimated PV potential results are compared to understand the PV efficiency considering meteorological conditions. In addition, building roof surface PV potential of Engineering Faculty of Anadolu University is calculated and the available roof area for PV installation is determined by using ArcGIS software.

Key Words: Solar radiation, PV simulation, Estimation, ArcGIS

ÖZET

PV DİZİLERİNİN MODELLENMESİ İÇİN GÜNEŞ IŞINIMI TAHMİNİ VE ArcGIS TABANLI GÜNEŞ ENERJİSİ POTANSİYELİ HESABI

Kübra BİTİRGEN

Elektrik-Elektronik Mühendisligi Anabilim Dalı

Anadolu Üniversitesi, Fen Bilimleri Enstitüsü, Haziran, 2018

Danışman: Yard. Doç. Dr. Ümmühan BAŞARAN FİLİK

Güneş enerjisi, en verimli alternatif enerji kaynaklarından biri olarak bilinir. Yeryüzüne ulaşan güneş ışınımı, güneş enerjisinin bir şeklidir. Güneş enerjisi uygulamaları, seçilen bölgenin güneş ışınımı potansiyeli hakkında tam bir bilgi ve ayrıntılı analiz gerektirir. Bu tezde, altı farklı güneş ışınımı hesaplama modeli kullanılarak Eskişehir için eğimli bir yüzey üzerinde saatlik küresel güneş ışınımı tahmin edilmiştir. Bu modellerin sonuçları, istatistiksel hata yöntemleri kullanılarak saatlik ölçüm verileri ile karşılaştırılmıştır. Tahmin sonuçları, modellerin performansını daha belirgin bir biçimde göstermek için aylık küresel güneş ışınımına dönüştürülmüştür. Uygun güneş ışınımı modeli seçildikten sonra, modeller karşılaştırıldığında, Eskişehir'in enerji potansiyelini hesaplamak için daha doğru sonuçlar veren model kullanılmıştır. MATLAB/Simulink programında ideal bir fotovoltaik panel simülasyonu uygulanmıştır, bunun yanı sıra, saatlik ölçülen rüzgar hızı, hava basıncı, küresel güneş ışınımı ve sıcaklık değerlerine dayalı olası PV panel enerji üretim miktarını hesaplamak için uygun bir algoritma seçilmiştir. PV potansiyelinin belirlenmesinden sonra, ideal PV simülasyonu ve tahmini PV potansiyeli sonuçları meteorolojik koşullar dikkate alınarak PV verimliliğini anlamak için karşılaştırılmıştır. Ayrıca, Anadolu Üniversitesi Mühendislik Fakültesi'nin bina çatı yüzeyinin PV potansiyeli hesaplanmış ve PV kurulumu için uygun çatı alanı ArcGIS yazılımı kullanılarak belirlenmiştir.

Anahtar Kelimeler: Güneş ışınımı, PV simülasyon, Tahmin, ArcGIS

ACKNOWLEDGEMENT

STATEMENT OF COMPLIANCE WITH ETHICAL PRINCIPLES AND RULES

I hereby truthfully declare that this thesis is an original work prepared by me; that I have behaved in accordance with the scientific ethical principles and rules throughout the stages of preparation, data collection, analysis and presentation of my work; that I have cited the sources of all the data and information that could be obtained within the scope of this study, and included these sources in the references section; and that this study has been scanned for plagiarism with "scientific plagiarism detection program" used by Anadolu University, and that "it does not have any plagiarism" whatsoever. I also declare that, if a case contrary to my declaration is detected in my work at any time, I hereby express my consent to all the ethical and legal consequences that are involved.

....

Kübra BİTİRGEN

TABLE OF CONTENTS

LIST OF FIGURES

LIST OF TABLES

NOMENCLATURE

G_{sc}	:	Solar radiation constant 1.367 (kW/m^2)
H_0	:	Extraterrestrial solar irradiation $(kWh/m^2 - hour)$
σ	:	Declination angle $(degree)$
ϕ	:	Latitude of the zone $(degree)$
ω_1	:	Sunrise hour angle $(degree)$
ω_2	:	Sunset hour angle $(degree)$
N	:	Day of the year $(unitless)$
ST	:	Solar time $(hour)$
LT	:	Local standard time $(hour)$
ET	:	Equation of time (min)
L_L	:	Local longitude $(degree)$
L_s	:	Standard time meridian $(degree)$
H_m	:	Measured global solar radiation on horizontal surface $(kWh/m^2 - hour)$
H_b	:	Direct solar radiation on horizontal surface $(kWh/m^2 - hour)$
H_d	:	Diffused solar radiation $(kWh/m^2 - hour)$
K_T	:	Hourly clearness index $(unitless)$
k_d	:	Hourly diffuse fraction $(unitless)$
H_T	:	Total global solar radiation on sloped surface $(kWh/m^2 - hour)$
$H_{T,b}$	:	Direct solar radiation on sloped surface $(kWh/m^2 - hour)$
$H_{T,d}$	:	Diffused solar radiation on sloped surface $(kWh/m^2 - hour)$
$H_{T,r}$	:	Reflected solar radiation on sloped surface $(kWh/m^2 - hour)$
r_b	:	Direct radiation conversion coefficient $(unitless)$
ρ_g	:	Ground reflectance coefficient $(unitless)$
A_i	:	Anisotropy index $(degree)$
f	:	Modulating function $(unitless)$
f_{c-s}	:	View factor for diffused radiation $(unitless)$
β	:	Slope angle $(degree)$
ω_s	:	Hour angle $(degree)$

θ	:	Angle of incidence (*degree*)
θ_z	:	Zenith angle (*degree*)
I	:	Output current of the PV array (A)
V	:	Output current of the PV array (V)
I_{pv}	:	PV current of the PV array (A)
I_o	:	Saturation current of the PV array (A)
n	:	Ideality factor of the diode (*unitless*)
V_t	:	Thermal Voltage (V)
k	:	Boltzmann's constant (J/K)
q	:	Electron charge (*coulomb*)
$I_{pv,n}$	:	Light-generated current at standard condition 25^oC (A)
I_{sc}	:	Short-circuit current (A)
$I_{sc,n}$	:	Nominal Short-circuit current (A)
I_{mp}	:	Current at the maximum-power point (A)
V_{oc}	:	Open-circuit voltage (V)
$V_{oc,n}$	:	Nominal open circuit voltage data sheet (V)
V_{mp}	:	Voltage at maximum-power point (V)
P_{mp}	:	Power at maximum-power point (W)
N_s	:	Number of cells in series in PV (*unitless*)
N_p	:	Number of cells in parallel in PV (*unitless*)
N_{ss}	:	Total number modules in the series (*unitless*)
N_{pp}	:	Total number modules in the parallel (*unitless*)
R_s	:	Series resistance in PV (Ω)
R_p	:	Parallel resistance in PV (Ω)
$P_{max,m}$	:	Calculated maximum power (W)
$P_{max,e}$	:	Maximum actual peak output power (W)
Δ_T	:	Difference between the nominal and measure temperature (^oC)
Δ_t	:	Temperature difference obtained from data sheet (^oC)
T	:	Actual temperature for ideal PV simulation (^oC)
T_c	:	Cell temperature inside module (^oC)
T_n	:	Nominal cell temperature (^oC)
T_m	:	Back-surface module temperature (^oC)

T_a : Measured ambient air temperature (^{o}C)

G_n : Nominal solar radiation, generally 1000 (W/m^2)

G : Actual solar radiation on PV for simulation (W/m^2)

$\sigma(T_c)$: Thermal voltage per each cell at temperature T_c (*unitless*)

WS : Wind speed measured at standard 10-m height (m/s)

a, b : Coefficients from PV array data sheet (*unitless*)

a_{Isc} : Short circuit current coefficient ($A/^{o}C$)

a_{Imp} : Maximum current coefficient ($A/^{o}C$)

β_{Voc} : Open circuit voltage coefficient ($V/^{o}C$)

β_{Vmp} : Maximum voltage coefficient ($V/^{o}C$)

a_0–a_4 : Coefficients of air mass factor (*unitless*)

M : Air mass depend on θ_z and air pressure (*unitless*)

M_{st} : Standard air mass (*unitless*)

P : Measured air pressure ($mmHg$)

P_o : Nominal pressure 760 ($mmHg$)

AOI : Angle between the sun and module degrees (*degree*)

b_0–b_5 : Incident angle coefficient (*unitless*)

c_0, c_1 : Coefficients regarding I_{mp} to effective solar radiation (*unitless*)

c_2, c_3 : Coefficients regarding V_{mp} to effective solar radiation (*unitless*)

1. INTRODUCTION

This Chapter is divided into three parts. In Section 1.1, background information of solar energy calculation models is given. The aim of this thesis is explained in Section 1.2. In Section 1.3, subjects of following Chapters are clarified.

1.1. Literature Review

With the technological and economical growth, energy requirements drastically increase by virtue of the shortage of traditional energy sources [1]. Currently, the increment of energy demand force us to search alternative energy sources. However, there are many types of renewable energy sources to replace the nonrenewable sources and the more available and nearly infinite source is solar energy. Solar energy has a large application field, for instance, PV systems converting solar energy into electricity, solar lighting, solar cars, solar power satellite, solar thermal electric power plants and etc.

One of the most challenging problems is how to determine the solar energy potential on a place before installing solar panels. Therefore, there are a number of studies assessing whether solar energy potential meets energy demand of the region or not. The efficiency of PV system mostly depends on the incoming solar radiation. To install the efficient PV system in a specific field, reliable and correct information is required. Additionally, solar radiation data is significant to identify the system design and availability of the PV system [2].

However, solar radiation measured data for a specific field is limited for many regions, especially in rural and mountainous surfaces. Incoming solar radiation on the Earth's surface is effected by a number of factors which are meteorological characteristics of a region [3]. There are many parameters for calculating and modeling the solar radiation such as meteorological parameters; cloudiness, ambient temperature [4, 5], humidity [6], sunshine duration [7, 8] and atmospheric pressure. Furthermore, there are a certain number of methods to calculate solar radiation by considering more than one effective factor. As in [9, 10], measured ambient temperature, sunshine duration are associated with the solar radiation. In [11], established a model named Bristow–Campbell to estimate daily solar irradiation from highest and lowest temperature values. In [12], the Bristow–Campbell model is reformulated

and measured data of solar radiation, precipitation, humidity, and temperature from different surfaces and climates are used for 40 stations to estimate daily solar irradiation.

Solar radiation is divided into two parts; global solar radiation that is below the atmosphere and extraterrestrial solar radiation that is above the atmosphere [13]. According to the angle of the surface, global solar radiation has two types which they are horizontal and tilted global solar radiation. The global solar radiation on a tilted surface covers three components: beam, diffuse from all part of the sky and reflected radiation from the ground. The reflected and direct radiation calculations are simple but the diffuse radiation is rather complicated. The diffuse radiation calculations need data related to global and direct radiation incident on a horizontal surface [14].

Meteorological information usually includes the total amount of radiation falling on a horizontal surface. However, the solar collectors usually have a certain angle placed. Therefore, determination of the amount of solar radiation coming to the inclined surface is vital importance in PV applications. The tilt angle is significant to indicate the amount of solar radiation potential but the only single tilt angle value is not valid for all the year because it differs with the earth rotation. According to [15], latitude angle should be taken as tilt angle to obtain the highest energy all the year. Furthermore, there is a study that explains the relationship between the optimum tilt angle and latitude by establishing a simulation resulted in the optimum tilt angle with a high accuracy 99.87% [16]. The study reaches an opinion for 35 places in Mediterranean Region that gives an average percentage reduction in the yearly solar radiation of only 0.016% if compared with real optimal tilt angle. In fixed tilt angle based latitude [17], six models which are isotropic or anisotropic models are compared by controlling the accuracy of the results in statistical tests.

Isotropic and anisotropic are the types of mathematical solar radiation prediction models on a tilted surface. Isotropic models are more available for hot and arid locations [18]. Liu and Jordan, Hottel and Woertz, Jimenz and Castro, Badescu, Tian et al and Koronakis introduced a number of isotropic models. With the intent of improving the accuracy of the isotropic models, the anisotropic models

are introduced by some researchers. The solar radiation estimation using these methods generally yields higher results in comparison to the isotropic models. Hay and Davies, Klucher, Reindl et al, HDKR (Hay-Davies-Klucher-Reindl), Temps and Coulson, Perez et al are some of the anisotropic models and assumed anisotropic methods [19].

In [20], Liu Jordan model is proposed as a isotropic model based three main parts of global solar radiation which are diffuse, direct and reflected. Kronakis model is also an isotopic model and proposed in [21]. As in [22], presented the Badescu model and differs from the Liu Jordan model in diffuse solar radiation calculation. Diffuse radiation components become more of an issue in Hay and Davies model included a circumsolar and isotropic component [23]. Well adapted algorithm of global solar radiation Reindl [24] presented a model which regards the modulating factor and all components of diffuse solar radiation on a tilted surface. In addition to circumsolar radiation and isotropic diffuse solar radiation, Hay and Davies, Klucher, Reindl et al, HDKR (Hay-Davies-Klucher-Reindl) model composed of three models [25]. It is deduced from the study [26] that Klucher model should be preferred for the estimation of global solar radiation on a tilted area. As in [27], the anisotropic based Hay and Davies model and Reindl model are recommended to estimate solar radiation for a south-oriented module. In [19], Hay and Davies model are found to be accurate for the estimation of global solar radiation on a tilted area. Also in [28], the two models that are indicated to be the most available models which are the Koronakis and Liu-Jordan to estimate diffuse solar radiation on tilted surface.

The isotropic and anisotropic models gives different estimation results. Hence, it is necessary to compare these methods with the aid of some validating methods. These methods supplies an idea that is related with the accuracy of the model used for estimation study. Methods used in validating the results: RMSE, MBE, MAPE and also t-statistic are statistical error parameters. The comparison can be made between the actual data and result of estimation by using the statistical methods [29, 30]. The statistical error parameters allow a benefit of understanding whether the models give statistically accurate or not at a particular reliable results.

To determine the solar radiation potential, geographical parameters latitude, altitude, and longitude are used [2]. In urban surfaces, there are some available pro-

posed methods and geo-referenced urban fabric models with regard to solar radiation tools to obtain solar radiation in different time scales. ArcGIS Solar Analyst [31] and Grass r.sun [32] are well known examples of this field. In [33], a method is proposed for associating ArcGIS with TRNSYS that provides an utilization of three ArcGIS tools, Spatial Analyst, Tracking Analyst and 3D Analyst modeling to enables a PV potential application using topographical data. However, Solar WebGIS is another application that is a web program with tools associated with mapping and extracting illustrator features on structures [34]. In [35], a study is carried out to obtain PV potential of rooftop surfaces for North-Western Italy. The [36] study presents a method to combine the properties of geographic information systems and image extraction to indicate the available rooftop surface for PV installation in Ontario.

Many of the existing methods use remote sensing data and GIS tools for assessment of accurate PV potential for large-scale areas [37, 38]. Remote sensing and GIS have a significant role, regardless of the scale of the application from individual to rural surface [39]. However, generally solar radiation models performed in GIS are available to use only for 2-D surfaces. The [40] proposed v.sun module using 3-D vector measured data visualising complex surfaces. By representing spatial visualization in [41, 42] , roof, facades and ground modeled as 3D objects to answer the question of whether the solar energy system to be intended to install can be adequate or not. In some studies [43, 44], the yearly solar irradiation over roof surface, regarding surface aspect and tilt angle are determined. Also as stated in [45], a LiDAR-based approach is proposed to determine the solar radiation incident on facades and roofs of buildings at city scale. The study involves a method for solar radiation calculation and performance evaluation of the proposed method . There is an improved study based on ArcGIS that covers many important factors relative to the solar radiation. Latitude, time of day, time of year, average climatic conditions, shading from nearby buildings and trees and surface orientation and slopes are considered for calculation of annual solar radiation on roof surface in [46] .

Solar radiation can be minutely, hourly, daily, monthly or generally yearly calculated [47]. The monthly average daily global solar radiation estimations for various locations are presented in different studies [48].

And there are also a number of studies in the literature using Artificial Neural

4

Networks(ANN) to calculate the solar radiation. In [49], a study is conducted to estimate daily solar radiation by using the minimum and maximum temperature values for desert areas. In [50], solar radiation considering air temperature and monthly mean daily value of global solar radiation are calculated. In [4] using air temperature values, Bayesian neural network (BNN) model, and empirical models are combined and this combination is improved to estimate daily global solar irradiation on a horizontal field. In [7], there is an improved model and a comparison between the eight combined and two single sunshine-based empirical models to estimate daily global solar radiation in humid areas. Due to the results of [51], in studies related to daily global solar radiation calculations SVM technique is superior to the ANN and ANFIS methods in humid surfaces. The studies [52, 53] are not related with the meteorological parameters and which are related the only day of the year.

To obtain usable energy from solar radiation, PV systems are used. PV array presents essential power conversion unit of a PV system. The application results of PV array is effected by solar radiation and cell temperature. PV array has nonlinear construction property. Before the design of the PV module, it requires the simulation of the model and maximum power point tracking (MPPT) for PV panel [54]. The general way for simulation of a PV array is for understanding the p-n junction working principle [55]. A PV model has a non-linear I-V property that is designed by current sources, diode(s) and resistors. To establish a PV simulation, it is necessary to model the single-diode or double-diode circuits. The single-diode model is easily applied to PV model correctly and clearly. Data sheet gives input values of PV models parameters by identifying important points in its I-V graph [56]. In addition, single-diode model can be implemented in many studies because of the basic construction consisted of single current source and diode [57, 58]. The model is available for power electronics designs. Some studies design more applicable methods that show more available precision for instance, an extra diode is added to present influence of the recombination of carriers [59, 60]. In [61], an improved modeling for the two-diode model of PV module is proposed. The fundamental contribution of the study is the simplification of the current formula, in which only four parameters are required, compared to six or more in the former two-diode models. Another study defines a three-diode model covered the effects of some parameters [62]. A PV array

study [63] explains a developed algorithm concerning the load following performance of the PV system under different conditions of ambient temperature and and solar radiation. The study considers in the event of loss of grid power by virtue of sudden faults and scheduled maintenance. In [64] a PV array simulation model is developed and implemented in Matlab-Simulink GUI environment. The model has PV basic circuit equations considering the effects of temperature and solar radiation changes. There is an available experimental research supplies a detailed information of the PV module and array performance model improved at Sandia National Laboratories for twelve years [65].

1.2. Thesis Aim and Objectives

There are three main purposes of this study. Firstly, comparative study of global solar radiation allows the selection of valid model for the studied surface. For this comparison six different solar radiation models which are currently used in many studies. The comparison carried out regarding to the statistical performance indicators. After the statistical results are compared with experimental results, selected model is used to calculate the possible generated power of PV system to be install.

Secondly, to understand the ideal performance of the PV panel, MATLAB simulation related with the PV panel is implemented. In addition, an improved PV circuit-based algorithm is selected to adjust the simulation and this method is tested. In this direction, the hourly solar radiation for all the year is determined and the possible power generation of the PV module is determined by using measured data which are temperature, air pressure and wind speed. The outcome of this PV simulation gives a possible generated power of PV system in Eskişehir regarding the selected PV model.

Thirdly, ArcGIS provides an opportunity to figure out how solar radiation coming to a certain surface by considering topographical characteristic of structures. The studied area is İki Eylül Campus of Anadolu University, Eskişehir. Slope and aspect angle calculations are available to obtain an accurate results for a horizontal plane or a tilted roof. The study covers an ArcGIS application to determine the yearly solar radiation. This program displays a surface considering elevation and

coordinates of the studied area that is more close to actual surface position. This part of thesis describes a model for prediction of solar energy potential. In order to evaluate this potential, a high-resolution orthoimage and DSM are modeled and annual solar radiation maps included direct and diffuse solar radiations are generated at ArcGIS Solar Analyst tool. Then, aspect, site latitude and optimal tilt angle factors are considered in indicating of PV panel location. The study assessing where solar panels should be install can considerably benefit PV performance.

1.3. Organization of Thesis

In Chapter 2, significant background material and methods are explained. To calculate hourly global solar radiation, six different models are presented in Section 2.1. In Section 2.2, an ideal PV panel simulation model and its characteristics are clarified. Furthermore, hourly solar radiation calculation of Badescu model used in PV model is presented.

In Chapter 3, ArcGIS program and its beneficial topographical tools are explained, and also slope and aspect maps are presented.

In Chapter 4, the estimation and simulation results of global solar radiation are shown. The most efficient solar estimation model is selected by considering statistical performance indicators in Section 4.1. In Section 4.2, ideal PV simulation model results and calculated PV potential are evaluated. In Section 4.3, PV potential for İki Eylül Campus of Anadolu University is calculated by using ArcGIS maps.

In Chapter 5, the study results are evaluated and remarkable points are discussed.

2. SOLAR RADIATION ESTIMATION FOR MODELLING OF PV ARRAYS

This chapter consist of two main parts. In the first part, six different global solar radiation estimation models and performance controlling methods are explained in this Chapter. In the second part, ideal PV array simulation is build in MATLAB/Simulink and the other PV simulation is implemented by using Badescu model and different PV algorithm.

2.1. Solar Radiation Estimation

Total monthly global solar radiation is estimated by using different models and statistical error parameters to identify the accuracy of these models. These models depend on the calculation of total monthly solar radiation from computing hourly solar radiation. Therefore, the results of hourly global solar radiation is summed up to obtain monthly global solar radiation. The reason of calculating monthly global solar radiation is to show the comparison results accurately.

2.1.1. Global Solar Radiation on Horizontal Surface

Calculating the amount of possible radiation on a horizontal surface of the Earth is a significant factor in solar applications. In [66], hourly extraterrestrial solar radiation on horizontal surface H_o calculation components; Solar constant ($G_{sc} = 1.367kW/m^2$), declination angle σ, latitude of the zone ϕ, sunrise hour angle ω_1, sunset hour angle ω_2 and number of the day N. Hourly extraterrestrial solar radiation which is evaluated by using the following Eq (2.1) that is widely preferred in many studies for hourly solar radiation calculations.

$$H_o = \frac{12x3600}{\pi}G_{sc}\left(1 + 0.033cos\left(\frac{360N}{365}\right)\right)(cos\phi cos\sigma(sin\omega_2 - sin\omega_1) + \quad (2.1)$$

$$\frac{\phi(\omega_2 - \omega_1)}{180}sin\phi sin\sigma)$$

The hour angle depends on the Earth rotation and it differs 15° angle per hour and following time equations are clarified in [28]. The sign of Eq (2.2) should be minus when the sunrise time is calculated, while it should be plus if the sunset time is required to determine. ω_1 and ω_2 are the hour angles at the beginning and end of the time interval.

$$\omega_1 = 15(12 - ST) \qquad \omega_2 = 15(12 + ST) \tag{2.2}$$

Solar time (ST) can be obtained from the Eq (2.3). LT is the local standard time and ET is the equation of time in minutes and calculated by below equation. L_L is the local longitude and L_s is the standard time meridian.

$$ST = LT + \frac{ET}{60} + \frac{4}{60}[L_s - L_L] \tag{2.3}$$
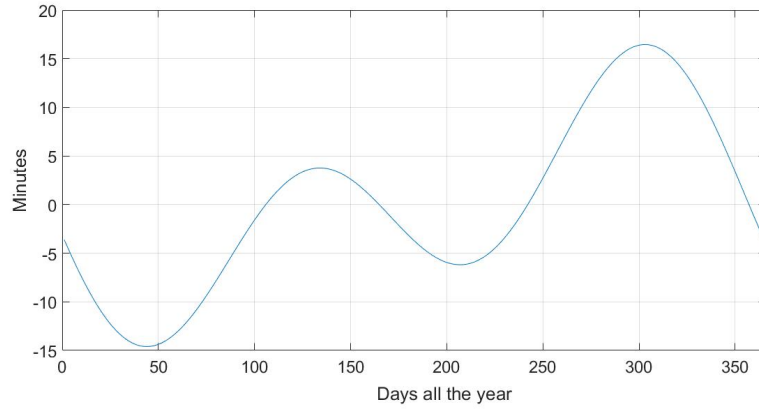
Figure 2.1. *Equation of time*

The ET is the relation of mean and the apparent solar times, both taken at a specific longitude at the same real time. ET is evaluated by the Eq (2.4). B is a parameter that is calculated for each day of the year represented in Eq (2.5). The calculated ET for Eskişehir is seen from the Fig 2.1.

$$ET = 9.87sin2B - 7.53cosB - 1.5cosB \tag{2.4}$$

$$B = \frac{360(N - 1)}{365} \tag{2.5}$$

The declination angle σ is computed for any day of the year using some empirical formulas by using Eq (2.6). Therefore, declination angle σ can be calculated based on the day of the year [67].

$$\sigma = 23.45sin\left(\frac{360}{365}(284 + N)\right) \tag{2.6}$$

To determine the optimum result, the hour angle has an importance on solar radiation calculations. Another equation that is Eq (2.7) providing the calculation of hour angle ω_s depending on the angle of latitude and declination angle. According to [1], ω_s is evaluated in the following formulas:

$$\omega_s = cos^{-1}(-tan\phi tan\sigma) \tag{2.7}$$

Hourly clearness index K_t is the ratio of the hourly measured global solar radiation H_m and extraterrestrial solar radiation H_o.

$$K_t = \frac{H_m}{H_o} \tag{2.8}$$

k_d is hourly diffuse fraction. This parameter is a topic of some studies by the virtue of the amount of global solar radiation changing in each location. Hence, there are many studies to determine the optimum value of the diffuse fraction. Because of this, Erb's formula is chosen in this study.

Erbs et al. conducted a study between 31° and 42° latitudes and its global and direct radiation obtained from 5 stations in the USA and diffuse radiation determined by the difference of these measured radiations. The k_d called diffuse fraction calculated in this study by using Erb's formula [68, 69]. H_d represents the diffused solar radiation on horizontal surface defined in below formula.

$$\frac{H_d}{H_m} = \begin{cases} 1 - 0.09K_t & K_t \leq 0.22 \\ 0.9511\text{–}0.1604K_t + 4.388K_t^2 - 16.638K_t^3 + 12.336K_t^4 & 0.22 < K_t \leq 0.8 \\ 0.165 & K_t > 0.8 \end{cases} \tag{2.9}$$

H_b is horizontal direct radiation and it is calculated as the difference of total daily radiation and diffuse radiation from the horizontal plane.

$$H_b = H_m - H_d \tag{2.10}$$

10

2.1.2. Global Solar Radiation on Tilted Surface

The total global solar radiation on the tilted surface can be determined with the help of various models in the literature. The total global solar radiation on sloped surface is calculated as the sum of the direct $H_{T,b}$, diffuse $H_{T,d}$ and reflected radiation $H_{T,r}$ [70]. The general formula is shown in Eq (2.11).

$$H_T = H_{T,b} + H_{T,r} + H_{T,d} \tag{2.11}$$

Direct solar radiation on a sloped surface $H_{T,b}$ calculation consists of horizontal direct solar radiation H_b and direct radiation conversion coefficient r_b expressed by Eq (2.12). θ_z is zenith angle, θ is angle of incidence and β is slope angle.

$$r_b = \frac{cos\theta}{cos\theta_z} = \frac{sin\sigma sin(\phi - \beta) + cos\sigma cos(\phi - \beta)cos\omega}{sin\sigma sin\phi + cos\sigma cos\phi cos\omega} \tag{2.12}$$

The θ_z and the θ can be computed by using Eq (2.13). The angle of incidence has more longer equation. The azimuth angle is considered as south facing oriented and it is evaluated by Eq (2.14).

$$cos\theta_z = sin\sigma sin\phi + cos\sigma cos\phi cos\omega \tag{2.13}$$

$$cos\theta = sin\sigma sin(\phi - \beta) + cos\sigma cos(\phi - \beta) \tag{2.14}$$

Some part of the incoming solar radiation that is reflected by any other intercepted material or the earth surface is named reflected radiation. Reflected radiation has a small portion of the global solar radiation. A lot of study ignores this component of solar radiation. On the other hand, this component is calculated by using different models in this study. Additionally, reflectance coefficient ρ_g is taken at 0.5 for dry locations.

Diffused radiation can be determined for all the isotropic models. Nevertheless, this coefficient equals different values for varied isotropic models thus this component is distinctive for each isotropic models.

Firstly, diffuse and direct solar radiation should be calculated for the horizontal surface. And then, reflected radiation can be obtained. After all, hourly total solar

11

radiation from the tilted surface can be calculated by the sum of direct, diffuse and the reflected radiation [71]. Hourly total solar radiation H_T is calculated by the following models.

2.1.3. Liu Jordan Model (LJ)

In this model, total solar radiation on tilted surface is expressed by the following equation. ρ_g is the surface reflectance ratio, and H_m is the total hourly solar radiation from horizontal surface. Liu Jordan model is an isotropic model and proposed in [20] and represented by following Eq (2.15).

$$H_T = H_b r_b + H_m \rho_g \frac{(1 - cos\beta)}{2} + H_d \frac{(1 + cos\beta)}{2} \qquad (2.15)$$

2.1.4. Badescu Model (BA)

Badescu model [22] has the view factor represented by $f_{c-s} = \frac{3 + cos2\beta}{4}$ which is the fraction of the diffuse radiation. The view factor f_{c-s} varies among these isotropic models. Total solar radiation calculation of this model is evaluated by using following equation:

$$H_T = H_b r_b + H_m \rho_g \frac{(1 - cos\beta)}{2} + H_d \frac{(3 + cos2\beta)}{4} \qquad (2.16)$$

2.1.5. Koronakis model (KO)

Kronakis model [21] is also an isotropic and has view factor f_{c-s} seen Eq (2.17). The calculation of total global solar radiation on inclined surface is simple as other isotropic models. And the three isotropic models has also same equation for calculation of direct and and reflected radiation. The difference between these isotropic models is the calculation of the diffuse radiation.

$$H_T = H_b r_b + H_m \rho_g \frac{(1 - cos\beta)}{2} + H_d \frac{(2 + cos\beta)}{3} \qquad (2.17)$$

2.1.6. Hay and Davies model (HD)

Hay and Davies model [23] is an anisotropic model. This anisotropic model includes the multiplication of the anisotropy index A_i and r_b. Furthermore, this model differs from the isotropic models due to diffuse solar radiation calculations. A_i is called anisotropy index and this parameter is determined by Eq (2.19).

$$H_T = (H_b + H_d A_i)r_b + H_m \rho_g \frac{(1 - cos\beta)}{2} + H_d \frac{(1 + cos\beta)}{2}(1 - A_i) + A_i r_b \quad (2.18)$$

$$A_i = \frac{H_b}{H_o} \quad (2.19)$$

2.1.7. Reindl et al. model (RE)

Reindl [24] model has also A_i and $f = \sqrt{\frac{H_b}{H_m}}$ modulating function of diffuse radiation intensity. Some diffuse radiation components are added to this model and this global solar radiation calculation is shown by Eq (2.20).

$$H_T = (H_b + H_d A_i)r_b + H_m \rho_g \frac{(1 - cos\beta)}{2} + H_d \left[\frac{(1 + cos\beta)}{2}(1 - A_i)\left(1 + f sin^3\left(\frac{\beta}{2}\right)\right) + A_i r_b \right]$$
$$(2.20)$$

2.1.8. Hay and Davies, Klucher and Reindl models (HDKR)

This model [25] is a mixture of the three models and more derived from Hay and Davies, Klucher and Reindl models. This model equation nearly equals the Reindl model but it differs from the Reindl model because it has not included the f. Moreover, this model takes into account all diffuse parameters of diffuse radiation apart from modulating function f. Solar radiation calculation of HDKR model can be seen by Eq (2.21).

$$H_T = (H_b + H_d A_i)r_b + H_m \rho_g \frac{(1 - cos\beta)}{2} + H_d \left[\frac{(1 + cos\beta)}{2}(1 - A_i)\left(1 + sin^3\left(\frac{\beta}{2}\right)\right) + A_i r_b \right]$$
$$(2.21)$$

2.2. Modeling of PV Arrays

Solar radiation calculations are available to obtain the solar energy potential for a specific surface. In accordance with this purpose, it requires the knowledge about possible power to be generated from PV panels.

Modeling of a PV panel can be implemented by constructing a simulation including an equivalent electrical circuit of the PV panel. In this study two algorithms are selected to visualize the working principle and possible outputs of PV panel in standard test conditions and measured conditions. The first selected model can be effectively implemented in some studies [72, 73]. The model is obtained in different studies due to basic construction consisted of single current source and diode. The model is available for power electronics designs because of easy modeling of single-diode model.

In this study, PV simulation is established in ideal conditions and measured conditions. After the PV panel simulation is applied in MATLAB Simulink, second algorithm depended on Badescu model is selected to obtain the possible PV output at measured conditions. As a consequence, the two implementation results are compared.

2.2.1. Simulation of PV Arrays

The selected model that is adjusted to simulate the PV panel includes some parameters which require to be computed, based on the data sheet. An effective compromise between simplicity and accuracy is ensured in simulation of single-diode model. Fig 2.2 represents the single-diode model of the PV cell.
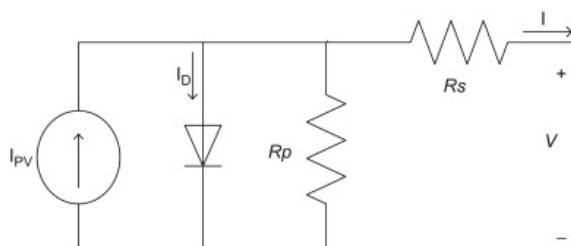
Figure 2.2. *Single diode model [62]*

The first Eq (2.22) of the simple PV panel does not include all information of the actual PV panel. As it can be seen from Fig 2.2, solar panels include the

number of parallel and series cells if these parameters are excluded, results does not compute with the data sheet curves. For this reason there is an improved model used in [72] and in this study this algorithm is implemented to Matlab/Simulink.

$$I = I_{pv} - I_o \left[\exp \frac{V + R_s I}{V_t n} - 1 \right] - \frac{V + R_s I}{R_p} \tag{2.22}$$

Output current of the PV represented I can be calculated by using Eq (2.22). I_o and I_{pv} are saturation and PV currents of the array and the studied circuit has thermal voltage represented by $V_t = N_s \frac{kT}{q}$. N_s is the number of series connected cells obtained from data sheet and n represents the ideality factor. The n which is the value of the diode constant can be randomly selected. Generally, this constant value differs from 1 to 1.5 and the selection belongs to other parameters of the I-V model. Some values for n are determined in [74] based on empirical analysis. In some studies the n value is determined by practical applications. The n constant has influence on the graph of current-voltage property. R_p is parallel resistance and R_s is series resistance of PV panel [60, 63].

As the PV array datasheet represented is observed, there is a few data about the PV array. Thus a lot of parameters which are necessary to implement the PV arrays is not known. For example, the information about PV current, the number of parallel cell, the diode reverse saturation current, and the band gap energy of the semiconductor are not added the data sheets. Generally, each data sheet has nominal short-circuit current $I_{sc,n}$, current at the maximum power point I_{mp}, maximum actual peak output power $P_{max,e}$, open-circuit voltage temperature constant β_{Voc}, short-circuit current temperature constant a_{Isc}, voltage at the maximum power point V_{mp}, nominal open-circuit voltage $V_{oc,n}$. All the constants are obtained from Table 2.1 but the β_{Voc} is calculated by using the Eq (2.40) defined in following section.

The R_p resistance is presented in the simulation circuit exactly so it belongs to the construction property of the PV cell. R_s is the equivalent series resistance of the PV panel. $G [W/m^2]$ is the solar radiation on PV, and G_n is nominal solar radiation. $I_{pv,n}$ is the light-generated current at the standard condition. Δ_T represents the temperature difference of the nominal temperature T_n and actual temperature T.

$$I_{pv} = G\left(\frac{I_{pv,n} + a_{Isc}\Delta_T}{G_n}\right) \tag{2.23}$$

The diode saturation current I_o and how the temperature effects the I_o is clarified in Eq (2.24). As modifying the below equation by [73], the single diode model of PV panel is improved.

$$I_o = \frac{I_{sc,n} + a_{Isc}\Delta_T}{\exp\left(\frac{V_{oc,n} + \beta_{Voc}\Delta_T}{nV_t}\right) - 1} \tag{2.24}$$

Maximum power calculation is included in iterative solution. Until it reaches the experimental maximum power value, the calculations continue. Calculated maximum power $P_{max,m}$ has evaluated in the Eq (2.25) and its calculation is not involved in the simulation:

$$P_{max,m} = V_{mp}\left(I_{pv} - I_o\left(\exp(\frac{q}{kT}\frac{V_{mp}R_sI_{mp}}{nN_s}) - 1\right) - \frac{V_{mp}R_sI_{mp}}{R_p}\right) = P_{max,e} \tag{2.25}$$

The Eq (2.26) shows the one step of iterative solution and this calculation continue until the calculated maximum power equals the measured maximum power.

$$R_p = \frac{V_{mp}(V_{mp} + I_{mp}R_s)}{V_{mp}I_{pv} - V_{mp}I_o\exp(\frac{q}{kT}\frac{V_{mp}R_sI_{mp}}{nN_s}) + V_{mp}I_o - P_{max,e}} \tag{2.26}$$

The model presents an iterative solution to compute the R_s and R_p parameters. After every iteration values of these parameters are observed, calculations are carried on until reaching the best result. In [73], proposed the below equation:

$$I_{pv,n} = I_{sc,n}\frac{R_p + R_s}{R_p} \tag{2.27}$$

Before obtaining the required value of R_s, it is assumed that the R_s equals zero because this coefficient is not given in data sheet of PV module. But R_p can be calculated by using the following formula:

$$R_{p,min} = \frac{V_{mp}}{I_{sc,n} - I_{mp}} - \frac{V_{oc,n} - V_{mp}}{I_{mp}} \tag{2.28}$$

16

This method has an importance due to the calculation of current I starting from 0 to obtain the actual value. The V increases proportionately to N_{ss} and the I remain unchanged. N_{ss} is the total number of modules within the series and N_{pp} is quantity of modules in parallel. Each array is comprised of N_{ss} x N_{pp} identical modules. The approach to compute PV current characterizing the I-V curve is as follows [72]:

$$I = I_{pv}N_{pp} - I_o N_{pp}\left[\exp\left(\frac{V + R_s I \frac{N_{ss}}{N_{pp}}}{V_t n N_{ss}}\right) - 1\right] - \frac{V + R_s I \frac{N_{ss}}{N_{pp}}}{R_p \frac{N_{ss}}{N_{pp}}} \qquad (2.29)$$

2.2.1.1. Application of PV Simulation

The PV array is constructed of a number of multiple PV cells. The PV module simulation represents the working principle of PV model. The simulink parameters are taken from the Fig 2.1. The simulation process starts with the implementation of the ideal PV panel simulation in MATLAB/Simulink. Therefore the outcomes of the PV panel simulation is determined at nominal condition. This simulation gives an advantage to show the effect of temperature and incoming solar radiation on PV power generation. In simulation part, ideal graphs are drawn to understand the optimum point of the voltages and currents of the PV panel. Fig 2.3 represents the PV panel simulation.

In contrast with the number of available datasheet of PV panels, each datasheet does not give the information of some parameter. The reason for this is the described iterative model is selected to calculate the unknown parameters. To realize a comparison between the nominal and estimated results, same data sheet type Schott SAPC 165 is used for simulations. These simulations are ideal PV simulation and the PV simulation considering Eskişehir meteorological data and estimated solar radiation. The selected data sheet Schott SAPC 165 has an information about the module characteristic curves at different radiation and temperature values.
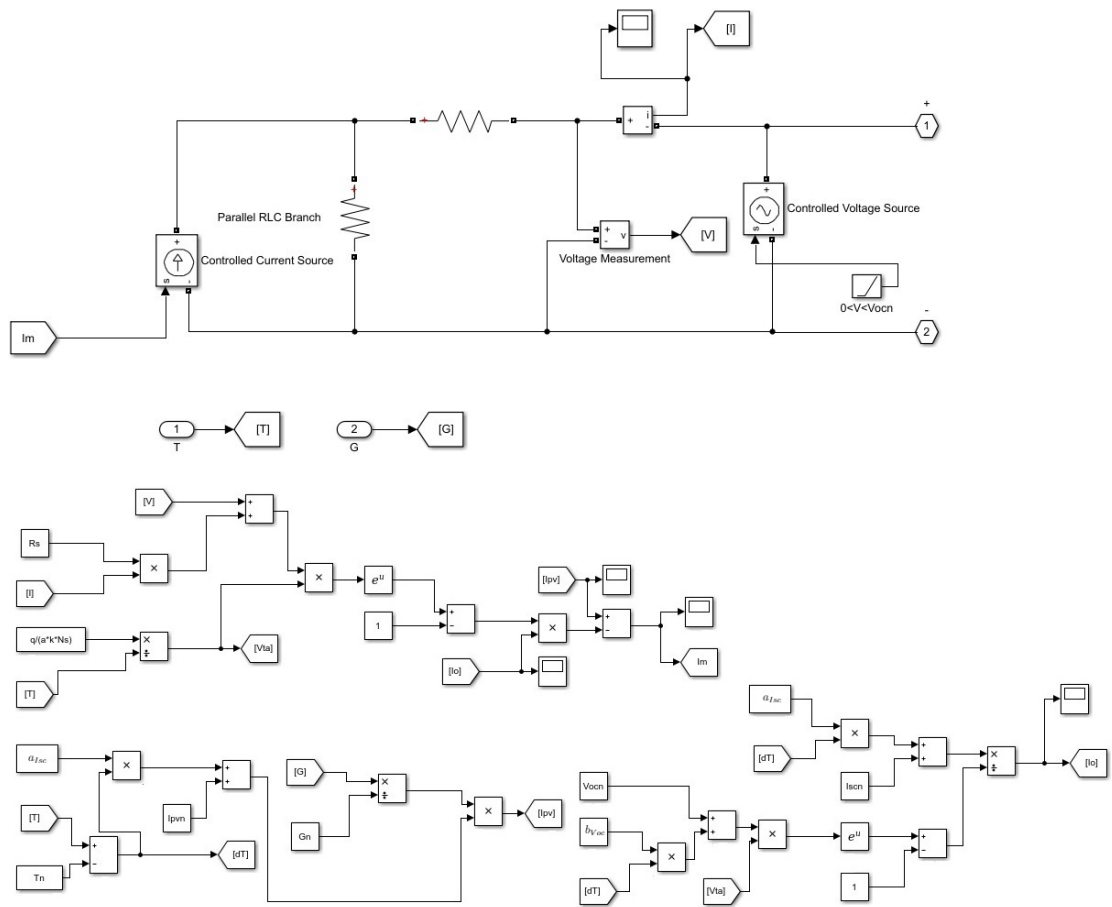
Figure 2.3. *PV circuit model constructed in MATLAB*

2.2.2. Badescu Model in PV Application

Global solar radiation on horizontal surface is clarified in section 2.1.1. For inclined surface solar radiation calculation is evaluated in section 2.1.2. Badescu model is explained in section 2.1.4 and the results of this model are used for this PV application.

The amount of air that solar radiation passes through the atmosphere M_{st}. It is called standard air mass that is determined by Eq (2.30). The improved formula for determination of the absolute air mass M shown in Eq (2.31) is comprised of air mass formula and can be computed as the multiplication of the airmass and the ratio of the atmospheric pressure and standard pressure at sea level [75]. P is measured pressure value of the studied area in Fig 2.4 for all the year in hour and P_o is a nominal value (760 mmHg).

18

$$M_{st} = (cos\theta z + 0.15(93.885 - \theta z)^{-1.253})^{-1} \qquad (2.30)$$

$$M = M_{st}\frac{P}{P_o} \qquad (2.31)$$
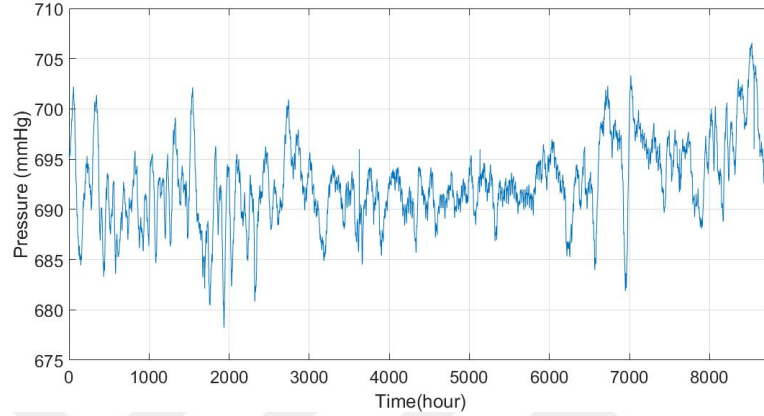
Figure 2.4. *Measured Pressure of the Eskişehir for all the year*

These functions $f_1(M)$ and $f_2(AOI)$ measure the effect on module short circuit current of inaccuracy in the solar spectrum and the losses derived from incidence of solar angle. These functions are indicated by a module testing procedures [76] [77]. AOI is the solar angle of incidence.

$$f_1(M) = a_0 + a_1M + a_2(M)^2 + a_3(M)^3 + a_4(M)^4 \qquad (2.32)$$

$$f_2(AOI) = b_o + b_1AOI + b_2(AOI)^2 + b_3(AOI)^3 + b_4(AOI)^4 + b_5(AOI)^5 \qquad (2.33)$$

2.2.3. Module Operating Temperature (Thermal Model)

The some effective factors of hourly global solar radiation are wind speed and temperature. Table 2.1 shows some important coefficient values. The Eq (2.34) gives the back surface module temperature T_m, H_T is the calculated global solar radiation depending on Badescu model, WS is the wind speed in (m/s) and T_a is the measured ambient air temperature. Fig 2.5 and Fig 2.6 represent the measured ambient temperature and wind speed in hour during the year in Eskişehir. a is the

coefficient that its value observed at highest module temperature, a certain amount of solar radiation and lower WS condition. b is a coefficient and its value related the module temperature which has inverse proportion with the WS.

$$T_m = H_T(e^{a+b.WS}) + T_a \qquad (2.34)$$
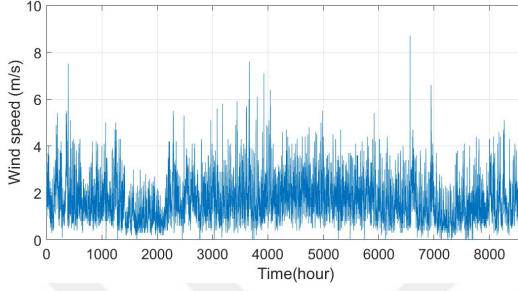
Figure 2.5. *Measured WS of Eski-*

şehir in hour for all the year
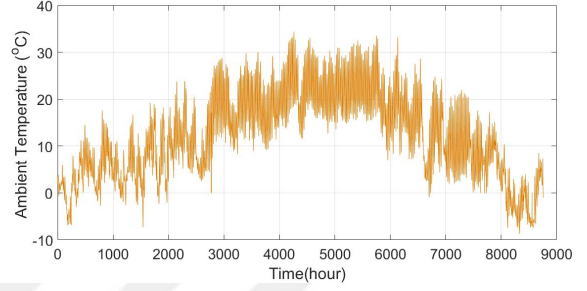
Figure 2.6. *Measured ambient tempe-*

rature of Eskişehir for all the year

Table 2.1. *Schott SAPC 165 type PV Module data sheet [66]*

Parameter	Value	Parameter	Value
$I_{sc,n}$	5.46	$\beta_{Voc,n}$	-0.171
$V_{oc,n}$	43.1	$m\beta_{Voc}$	0
$I_{mp,n}$	4.77	$\beta_{Vmp,n}$	-0.178
$V_{mp,n}$	34.6	$m\beta_{Vmp}$	0
C_0	0.988	a_{Isc}	0.00079
C_1	0.012	a_{Imp}	-0.00001
C_2	0.20456	n	1.486
C_3	-5.4788	N_s	72
A_0	0.938	N_p	1
A_1	0.052543	B_0	1
A_2	-0.0083131	B_1	-0.002438
A_3	0.00057776	B_2	0.0003103
A_4	-0.00001537	B_3	-0.00001246
a	-3.56	B_4	2.112e-07
b	-0.075	B_5	-1.359e-09

According to the [65], the cell temperature inside the module T_c is calculated

by Eq (2.35). Nominal solar radiation G_n equals generally 1000 W/m^2. The temperature difference is represented by Δt obtained from [78] and Δt is generally taken at 2 or 3 ${}^oC$ for a flat-plate module in an open-rack mount.

$$T_c = T_m + \frac{H_T}{G_n}\Delta t \tag{2.35}$$

The thermal voltage per each cell at temperature T_c is represented by $\delta(T_c)$. Eq (2.36) includes the Boltzmann's constant k, electron charge q and ideality factor of the diode n.

$$\delta(T_c) = \frac{nk(T_c + 273.15)}{q} \tag{2.36}$$

If the positive or negative power outputs of the panel are directly short-circuited without load, the flowing current which is short circuit current I_{sc} can be calculated by Eq (2.37). Horizontal direct solar radiation H_b, horizontal diffuse solar radiation H_d and extraterrestrial solar radiation H_o are clarified in prior sections and the values of these parameters are taken from the Badescu model solar radiation calculation result. As explained in PV simulation section, T_n is the nominal temperature and a_{Isc} represents the short circuit current temperature coefficient.

$$I_{sc} = I_{sc,n}f_1(AMa)((H_b.f_2(AOI) + fH_d)/H_o)(1 + \alpha_{Isc}(T_c - T_n)) \tag{2.37}$$

The formulations of current and voltage are clarified in [65]. The effective solar radiation E_e can be explained as the fraction of the I_{sc} and the different coefficients. The E_e is the solar radiation in the plane of the module to which the cells in the module actually respond, after the influences of solar spectral variation, module soiling and optical losses by virtue of solar angle of incidence are considered. It is calculated by using Eq (2.38).

$$E_e = \frac{I_{sc}}{I_{sc,n}(1 + \alpha_{Isc}(T_c - T_n))} \tag{2.38}$$

Maximum power point current tends to increase slightly with increment of the difference of the reference temperature and cell temperature inside the module. Maximum power point current I_{mp} at any operating condition can be simply calculated by solving the following Eq (2.39). For the below equation, maximum

21

power point current at nominal condition $I_{mp,n}$ and the other unknown parameters are obtained from the Table 2.1.

$$I_{mp} = I_{mp,n}(c_o E_e + c_1 E_e^2)(1 + \alpha_{Imp}(T_c - T_n)) \tag{2.39}$$

The temperature coefficient of open circuit voltage $\beta_{Voc,n}$ is experimentally measured at nominal conditions of module and $m\beta_{Voc}$ is a coefficient enabling a dependence on solar radiation. These parameters are used to calculate the temperature coefficient of open circuit voltage β_{Voc} in actual measured conditions and they are obtained from Table 2.1. The calculation of the β_{Voc} can be given as:

$$\beta_{Voc} = \beta_{Voc,n} + m\beta_{Voc}.(1 - E_e) \tag{2.40}$$

To obtain maximum voltage, maximum voltage temperature coefficient β_{Vmp} can be calculated similarly with the β_{Voc}. Thus, Eq (2.41) composed of two temperature coefficients which they are maximum voltage temperature coefficient $\beta_{Vmp,n}$ based nominal condition and $m\beta_{Vmp}$ supplying radiation dependence.

$$\beta_{Vmp} = \beta_{Vmp,n} + m\beta_{Vmp}.(1 - E_e) \tag{2.41}$$

The relation of solar radiation with the open-circuit voltage composed of a logarithmic function and some factors. Open circuit voltage V_{oc} of PV panel can be evaluated using Eq (2.42). N_s represents the number of cells in series in PV.

$$V_{oc} = V_{oc,n} + N_s \delta(T_c) ln(E_e) + \beta_{Voc}(E_e)(T_c - T_n) \tag{2.42}$$

Maximum power point Voltage V_{mp} has this Eq (2.43) using some of the data sheet constant factors.

$$V_{mp} = V_{mp,n} + c_2 N_s \delta(T_c) ln(E_e) + c_3 N_s (\delta(T_c) ln(E_e))^2 + \beta_{Vmp}(E_e)(T_c - T_n) \tag{2.43}$$

Maximum power P_{mp} is determined by multiplying maximum current and voltage shown in Eq (2.44).

$$P_{mp} = I_{mp} V_{mp} \tag{2.44}$$

3. CALCULATION OF SOLAR ENERGY POTENTIAL BASED ON ArcGIS

It is necessary to explain the ArcGIS program which is used to indicate the solar energy potential of Engineering Faculty, Anadolu University considering topographical characteristic and tilt angle. ArcGIS means Aeronautical Reconnaissance Coverage Geographic Information System. This program provides a unique set of capabilities to visualize and analyze a region.

On the purpose of determination of the solar potential of building roof for solar panel installation, initially availability of building roof surfaces are considered. Furthermore, ArcGIS program is an available application for geographic areas to be mapped for a certain times scale by using digital elevation model (DSM). In this study, the solar energy potential is predicted by using solar radiation model based on ArcGIS and the stages of this study is also clarified in [79].

Description of study area, determination of suitable building roof surface, tilt angle with aspect factors and calculation of solar energy potential are presented in this section.

3.1. Description of Study Area

The selected area is located at North Hemisphere, $39^{o}48'$ latitude and $30^{o}32'$ longitude. The region is selected by virtue of its characteristics which is not dominated by high rise buildings. The data is provided by the Institute of Earth and Space Science of Anadolu University, Eskişehir. Fig 3.1 represents the high resolution orthoimage of the Engineering Faculty of Anadolu University. DSM of the Faculty is shown in Fig 3.2. The 0.5 m resolution raster data is selected for a clear view to parcel building structures in this application. High resolution orthoimage displays the faculty and visualize the roof structures clearly.

3.2. Rooftop Area Estimation

DSM and high-resolution orthoimage which are interpolated with a spatial resolution of 0.5 meter are utilized to calculate the rooftop area in m^2. The DSM data shows not only the bare earth, but also it includes surface features like trees and building structures.

Figure 3.1. *Orthoimage of Engineering Faculty at İki Eylül Campus*
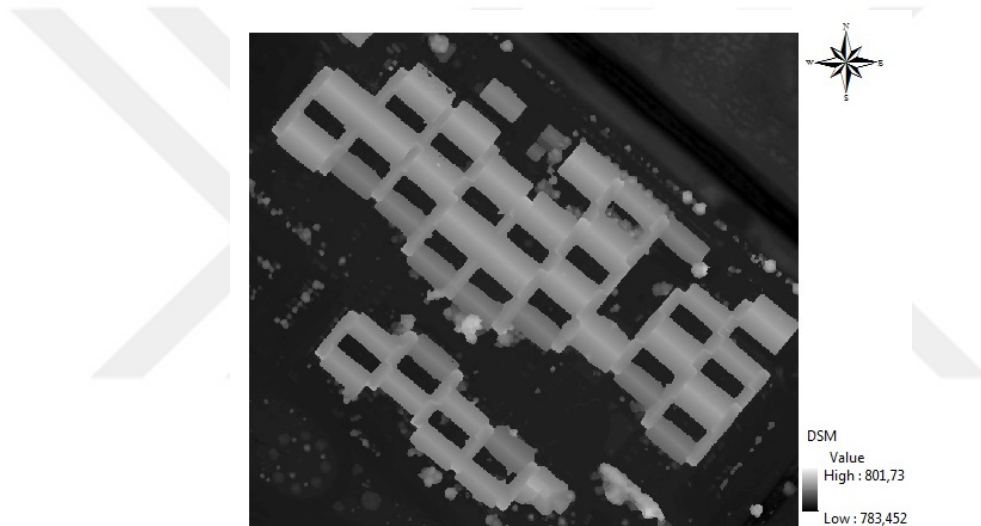
Figure 3.2. *DSM of Engineering Faculty at İki Eylül Campus*

Firstly, hemispherical viewshed based on topography is indicated by adjusted all the data sets to ArcGIS WGS 84. To digitize the roof dimension in parcels in the ArcMap, the roof area is extracted from high-quality building footprints. The roof shape is the a distinctive predominant factor separating building structure from other objects. To produce high quality segmentation result, the selected area is divided into the different five regions by area in order. The suitable roof area is calculated to be $13,320\ m^2$ by using ArcCatolog tool for this study area.

3.3. Tilt Angle and Aspect Factors

To indicate optimal sites based on multiple criteria for PV panel installation, panel tilt angle have been broadly thought. In this way, the tilt angle should be

determined using the specific geographic location and building height. On the other hand, the optimum tilt angle varies day by day, but this variation of angle throughout the year is not practical. Consequently, a fixed tilt angle for all the year or for a season in a specific surface is more applicable for PV installation. .

Figure 3.3. *Slope map of Engineering Faculty at İki Eylül Campus*

Slope map based ArcGIS is generated by using DSM. According to [80], available tilt angle is taken as the lower values of 35^0. In Fig 3.3, roof tilt angles of Engineering Faculty can be observed for all pixels of building rooftops. It is apparent that the tilt angles do not vary sharply and most of rooftops are suitable according to the assumed tilt angle for PV installation.

Figure 3.4. *Aspect map of Engineering Faculty at İki Eylül Campus*

Site selection is considering both tilt angle and aspect angle of the rooftop

surface. In this study aspect angle value is assumed to be $67.5^0 - 292.5^0$ since the south facing parts of the rooftops receive most amount of solar radiation [81]. It can be seen from Fig 3.4 that tilted south-oriented roofs receive more solar radiation than other parts of the rooftops of buildings according to the assumed angle interval.

In order to evaluate the results of the maps based two criteria for PV application, the overlay map is formed from roof surface slope and aspect of this location. To obtain the overlay map representing the most available rooftop surface, aspect and slope maps are reclassified and correlated. Fig 3.5 shows the availability of the rooftops in respect to geographical location and surface elevation.

Figure 3.5. *Overlay map of Engineering Faculty*

After reclassification process, resulted overlay map representing availability of building roof surface in the engineering faculty is shown in Fig 3.5. Areas shown in yellow are the available surfaces for this analysis. These results of this analysis have a weighted significance for site selection.

3.4. Solar Energy Potential Calculation

Solar energy potential calculation on a surface based on ArcGIS program has two main tools these are area solar radiation and point solar radiation. In this study, area Solar Radiation tool is handled. When building rooftops are identified then annual solar radiation maps are generated for that region. Therefore, it is essential to compile the results in order that energy potential on each selected roof

can be calculated. Energy potential calculation formula [82] is generally used in solar energy calculations and it can be defined as follows:

$$E = A.r.H.PR \qquad (3.1)$$

The solar energy potential E in kWh is evaluated by using Eq (3.1). A represents the total PV panel area in m^2. Additionally, the two parameters depend on the PV panel characteristic which are performance ratio coefficient PR and PV panel yield r. According to construction material and efficiency of PV panel, values of these parameters are selected from PV datasheet. Annual solar radiation H in kWh/m^2 is estimated in ArcGIS solar analyst tool.

4. RESULTS AND DISCUSSION

In this chapter, simulations and results are explained along with the some evaluation methods. In first study, four different statistical error indication methods are selected and implemented to understand the accuracy of the estimation results.

To understand the ideal PV potential, PV panel simulation is build in MATLAB/Simulink. After the selection, regarding the wind speed, pressure and temperature and also the measured solar radiation PV potential calculated for Eskişehir.

Last part, there is an application used ArcGIS and more detailed and specific for Engineering Faculty of İki Eylül Campus, Anadolu University.

4.1. Estimation Global Solar Radiation and Model Selection

By using the statistical error methods [83], estimated and measured hourly global solar radiation values are compared. Hence, accuracy of the aforementioned models is assessed to indicate the best model for the studied area. The MAPE is the mean absolute percentage error calculated from the measured value and values of the regression models. The MAPE is evaluated by using Eq (4.1). However, mean bias error (MBE) can be expressed as Eq (4.2) and supplies information on the long term performance of the correlation. In this assessment method, $Y_{i,m}$ is estimated, $Y_{i,c}$ is measured data and number of observations represented by n.

$$MAPE = \frac{1}{n} \sum_{i=1}^{n} \left| \frac{Y_{i,m} - Y_{i,c}}{Y_{i,m}} \right| .100 \qquad (4.1)$$

$$MBE = \frac{1}{n} \sum_{i=1}^{n} (Y_{i,m} - Y_{i,c}) \qquad (4.2)$$

$$RMSE = \sqrt{\frac{1}{n} \sum_{i=1}^{n} (Y_{i,m} - Y_{i,c})^2} \qquad (4.3)$$

$$t - stat = \sqrt{\frac{(n-1)MBE^2}{RMSE^2 - MBE^2}} \qquad (4.4)$$

Other statistical method root mean error (RMSE) shows that the model estimation performance. It takes always positive values and the ideal value is to be

zero. RMSE resembles MBE but the difference of these two types is that the RMSE taking square of the difference of the measured data and prediction result and calculating the square root of this result. One of the most widely used methods in study accuracy test, t-statistic shows the difference of the method and measured data and more. It also measures the performance of the models. Thus it can be decided whether the difference is random or statistical makes sense.

The object of this comparison is to select the more available model to calculate of the possible energy potential and use this model in simulation of PV module. When the results of this application is observed, the Badescu model has the least error and lower values of solar radiation and also closest to the measured value. The result of HD model has so high error results when comparing the other models.
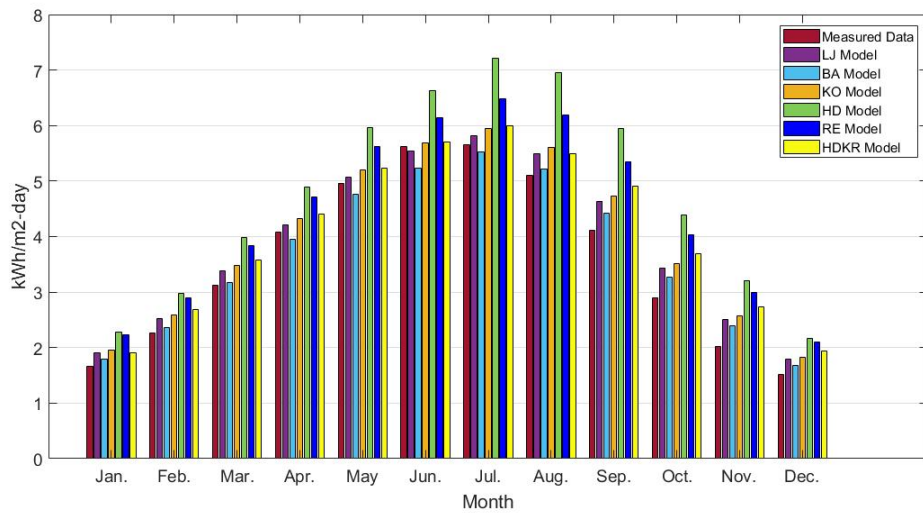
Figure 4.1. *Total Monthly solar radiation on tilted plane of Eskişehir*

Fig 4.1 represents a comparison of different models to estimate total monthly global solar radiation on tilted surface. It is necessary to clarify why the total monthly global solar radiation calculated for the model selection instead of using hourly global solar radiation values. To show the difference of the models results more specifically, monthly global solar radiation calculated by the sum of the hourly global solar radiation values. If the figure is observed, it is observed that the highest estimation is the anisotropic model HD. According to estimation results the most close to real value is the Badescu model.

One of the efficient statistical error test is MAPE evaluated following Table

and in this performance indication method shows the least error as Badescu model.

Table 4.1. *Statistical Error Methods Results*

| Months	Methods	LJ	BA	KO	HD	RE	HDKR
Jan.	MAPE	0,56	0,23	0,91	1,04	1,29	0,56
	MBE	0,12	-0,01	0,05	0,064	0,08	0,03
	RMSE	3,53	0,70	5,69	6,46	13,68	3,53
	t-statistic	0,03	0.0142	0.0087	0.0099	0.0058	0.0084
Feb.	MAPE	0,91	0,13	1,25	1,68	1,8	1,73
	MBE	0,48	0,01	0,095	0,12	0.13	0,10
	RMSE	1,08	1,94	9,55	6,78	44,96	10,80
	t-statistic	0,49	0.0005	0.0099	0.0177	0.0028	0.0415
Mar.	MAPE	2,16	1,55	2,05	4,71	3,87	2,85
	MBE	6.31	0,18	0,28	0,54	0,44	0,33
	RMSE	6,97	21,07	28,18	13,00	46,04	33,11
	t-statistic	0,03	0.0008	0.0099	0.0415	0.0095	0.0099
Apr.	MAPE	1,71	1,14	1,96	4,13	3,13	2,20
	MBE	6,33	0,16	0,28	0,60	0,46	0,32
	RMSE	25,12	50,35	28,81	59,62	55,76	32,33
	t-statistic	0,01	0.0031	0.0097	0.0415	0.0082	0.0098
May	MAPE	1,77	1,28	1,98	4,80	3,02	2,10
	MBE	10.69	0,23	0,36	0,88	0,55	0,38
	RMSE	25,17	49,46	36,58	141,47	51,78	38,77
	t-statistic	0,01	0.0046	0.0098	0.0062	0.0106	0.0098
June	MAPE	1,51	1,11	1,68	5,03	2,55	1,73
	MBE	9.42	0,22	0,34	1,02	0,51	0,35
	RMSE	32,70	39,25	34,20	158,98	66,45	35,15
	t-statistic	0,02	0.0056	0.0099	0.0064	0.0084	0.0099
July	MAPE	1,51	1,11	1,68	5,03	2,55	1,73
	MBE	21.18	0,39	0,48	1,45	0,66	0,50
	RMSE	30,70	22,62	48,97	145,98	78,10	50,84
	t-statistic	0,03	0.0172	0.0098	0.0099	0.0084	0.0098
Aug.	MAPE	2,91	2,60	3,05	8,36	4,10	2,91
	MBE	30.76	0,49	1,58	0,78	0,55	0.55
	RMSE	46,03	23,76	58,07	102,04	80,93	55,46
	t-statistic	0,03	0.0206	0.0272	0.0076	0.0067	0.0099
Sept.	MAPE	3,76	3,40	3,91	9,56	5,47	4,44
	MBE	30.97	0,50	0,57	1,41	0,80	0,65
	RMSE	55,46	16,79	57,95	88,69	45,96	65,68
	t-statistic	0,03	0.0297	0.0098	0.0002	0.0174	0.0098
Oct.	MAPE	2,60	1,95	2,88	5,52	4,26	3,36
	MBE	7,89	0.21	0,59	0,45	0,36	0.36
	RMSE	28,09	18,08	31,13	60,59	14,69	36,32
	t-statistic	0,03	0.0116	0.0189	0.0074	0.0245	0.0099
Nov.	MAPE	1,10	0,26	1,47	1,78	2,01	1,65
	MBE	0,65	0,01	0,10	0,13	0,14	0,12
	RMSE	8,07	1,01	10,73	54,73	8,18	12,04
	t-statistic	0,14	0.0099	0.0093	0.0023	0.0171	0.0099
Dec.	MAPE	0,68	0,12	1,03	1,20	1,45	1,17
	MBE	0,14	-0,01	0,05	0,06	0,08	0.06
	RMSE	3,83	1,45	5,80	12,81	8,02	6,61
	t-statistic	0,29	0.0068	0.0086	0.0046	0.0099	0.0091

An also there is an efficient statistical test MBE . This test not only indicates the error for this application but also is used to calculate t -statistic test. In addition, Table 4.1 also represents the MBE test results. It can be seen that the least error belongs to Badescu model.

RMSE is an efficient way of determining the error of an estimation. With reference to RMSE property, Badescu model has the lowest estimation error seen in the Table 4.1.

The t-statistic is more reliable compared to other tests. That covers RMSE and MBE statistical test and called t-statistic. If the Table 4.1 is observed, Badescu model has the lowest error results.

4.2. PV Simulation Result

To obtain the closest result with measured data, six different models are compared by fixing the tilt angle at 39.79^0 (latitude of Eskişehir). Results show that the highest output is HD model and lowest one is Badescu model. Hence, Badescu model is selected to calculate the PV panel efficiency since this model gets the lowest statistical error.
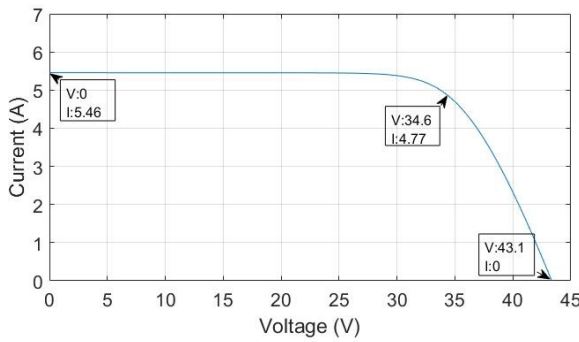
Figure 4.2. *Current versus Voltage graph on Photovoltaic simulation*
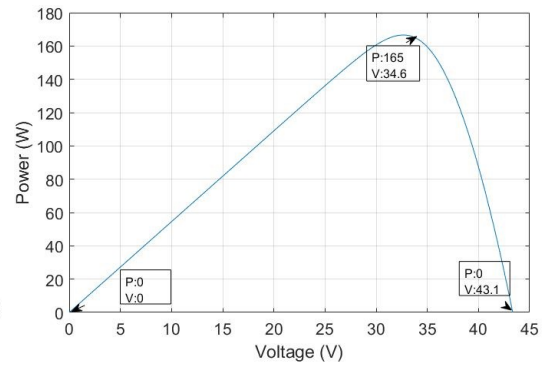
Figure 4.3. *Voltage versus Power graph on Photovoltaic simulation*

In first part of PV simulation, ideal graphs are drawn to understand the optimum point of the voltages and currents of the PV panel. The first two curves are composed for nominal conditions, that is to say, under the sunshine of $1000W/m^2$, the temperature of 25°. As in Fig 4.2, it can be understood that the short circuit
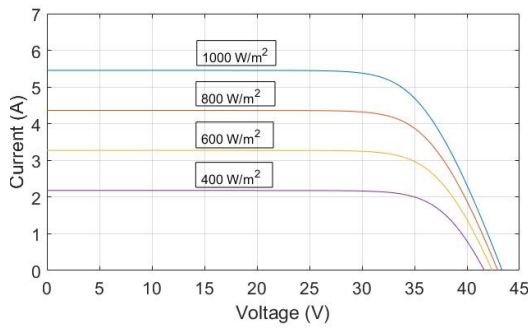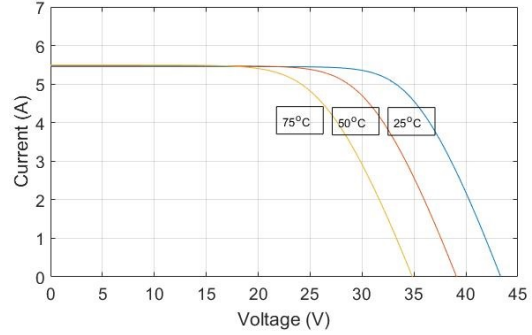
Figure 4.4. *Current versus voltage graph in varying solar radiation*

Figure 4.5. *Current versus voltage graph in varying temperature*

current and open circuit voltage are the extreme points of the I-V curve of PV module. Furthermore, Fig 4.3 represents the maximum power to be generated of PV module. According to Fig 4.4, the various solar radiation values on PV panel effects the generated voltage and current in fixed 25° temperature. The results of the temperature influence at constant solar radiation is shown in Fig 4.5. The simulation straightly demonstrates that the outcomes of PV module at nominal conditions.
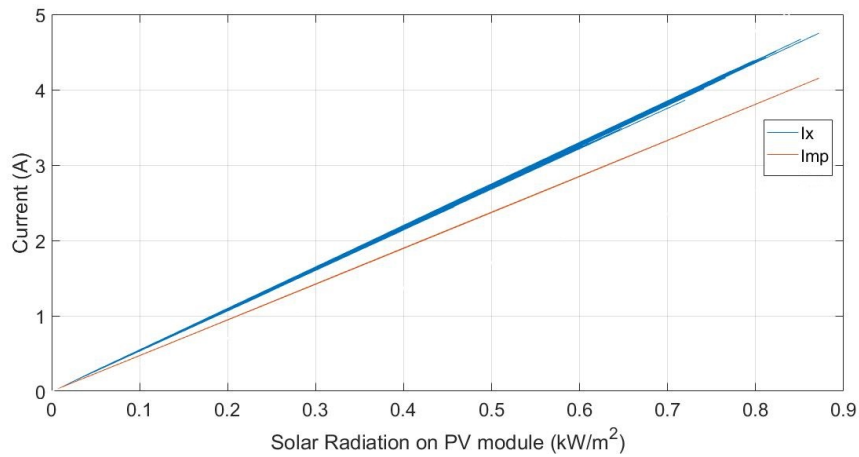
Figure 4.6. *Current on PV module versus solar radiation*

As mentioned in Section 2.2.3, hourly global solar radiation depending on the Badescu model is calculated to use the PV panel analysis. In PV panel study possible outcomes of PV module in Eskişehir is determined considering meteorological

criteria such as WS, temperature and air pressure. In addition, Fig 4.6 represents a graph of the maximum current and short circuit current versus calculated solar radiation on PV module. The currents tends to increase with increasing effective solar radiation. Moreover, voltage potential respect to effective solar radiation of PV module is shown in Fig 4.7. The result show that at starting point voltage increase but after that it comes to a state of stable condition due to PV characteristic.
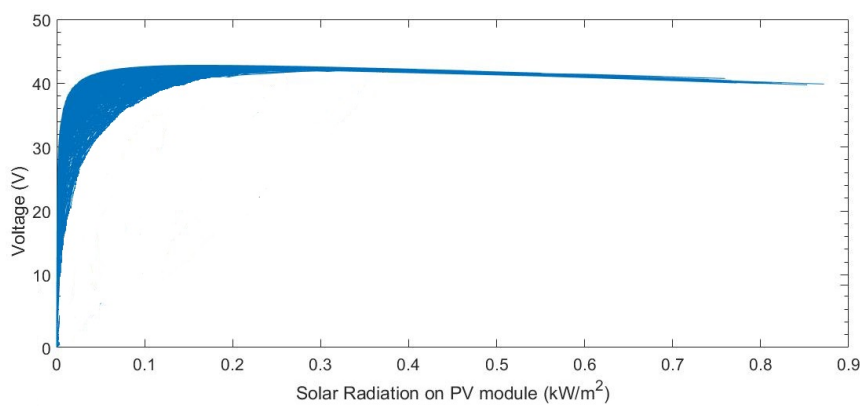
Figure 4.7. *Voltage on PV module versus solar radiation*

As in Fig 4.8, determined cell temperature and measured air temperature values can be seen. And also there is an increment of the cell temperature because Sun lights heats the PV module, this condition requires more detailed research and study in further. Inasmuch as this system requires cooling system. Some studies proposed that the water cooling systems improve the PV system performance [84, 85].

In Fig 4.9, prediction of PV generated Power from estimated solar radiation on tilted surface draw attention to the power reduction in the summer days. It is known that the highest amount of solar radiation values can be obtained in days which receives the most solar radiation and long sunshine hours but for higher values
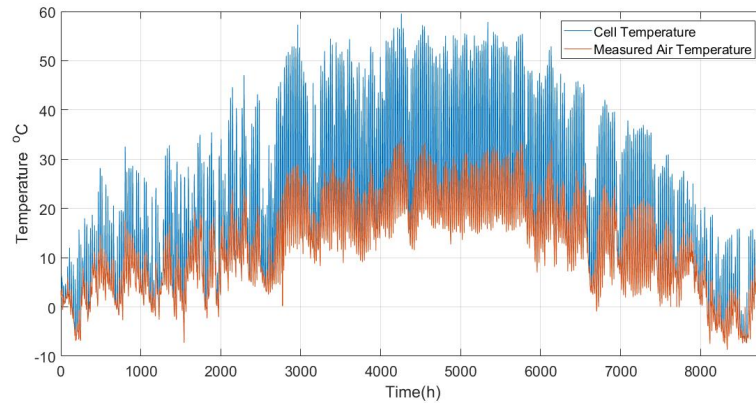
Figure 4.8. *Estimated PV temperature versus measured air temperature*

of temperature the PV panel efficiency decreases. Hence, the Fig 4.9 result validates that the temperature has an reducing effect on power generated from PV module due to heating effect. In addition, the selected PV panel has 12.7% efficiency [86].
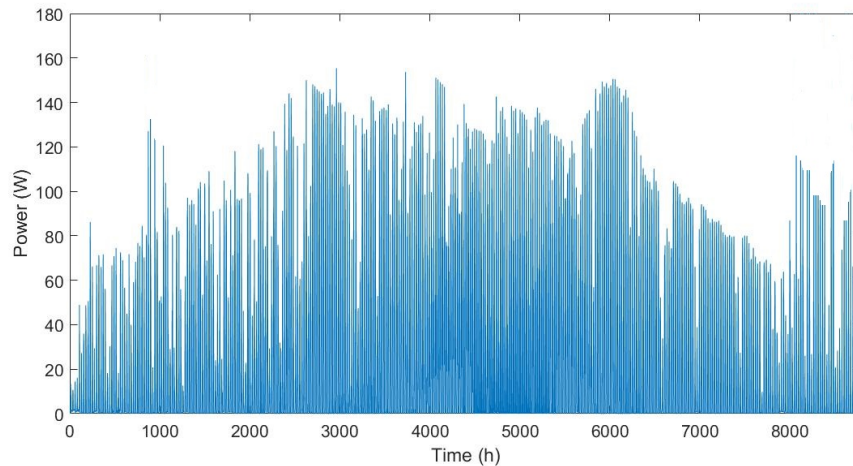
Figure 4.9. *Estimated Power values of selected solar panel*

As is known from ArcGIS study, available roof surface for PV installation is calculated for the Engineering Faculty. Therefore, the PV potential of the Faculty can be calculated by using this possible generated power result which is above. In addition, the PV potential of Engineering Faculty depending on the Badescu model is 2.01 MW. The result gives the total PV potential of the selected region and it provides an opportunity to compare the ArcGIS and Badescu model algorithms in

34

a distinctive perspective.

4.3. ArcGIS Application Results

The requirement for solar radiation analysis is to take into account geographical condition of the studied region. The object of these aforementioned models is to obtain solar radiation at a specific area but all these exclude the topographical characteristics of the area. However, there are lots of studies proposed ArcGIS and similar programs for PV potential calculations.

In this study, annual solar radiation estimated using ArcGIS based on the different data resources, such as elevation, aerial imagery and latitude. In an attempt to solar radiation calculation time scale is selected to one year and considered the meteorological sky conditions selected according to the seasons. For a very clear sky 0.2, general clear sky 0.3 and very cloudy sky conditions 0.7 value is selected in yearly solar radiation applications and the values are changed according to different meteorological conditions of Eskişehir.

Solar radiation map is generated for each point on the building roof with a spatial resolution of about 0.5 m. The calculation of total yearly solar radiation is resulted at 2.06 MW. While the PV potential of buildings are obtained, the particular property of the model used to detect the most favourable surfaces for the PV system installation. In this way, suitable roof surface is indicated as $13,320 \ m^2$ at ArcCatolog tool. As a result Fig 4.10 gives an informative look at annual solar radiation of the Engineering Faculty. The annual solar radiation map based pixel supplies a detailed information about total yearly solar radiation of studied area. The more red the pixel is, the more amount of solar radiation it receives but for yellow parts, this condition is opposite. The solar radiation value varies through the

map and within each roof.

If the two maps depended on slope and aspect are observe, these maps clarify that vertical roofs and north oriented parts have considerably less energy potential compared to other parts of building roofs.
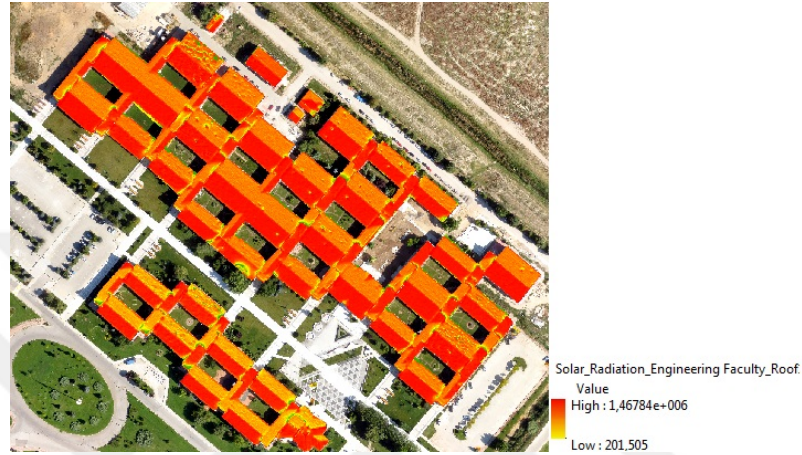
Figure 4.10. *Annual Solar Radiation of Engineering Faculty*

To indicate the number of PV panels, a 260 W panel of 1.62 m^2 is chosen which is currently used in the renewable energy research lab of İki Eylül Campus in Anadolu University. The selected PV panel has 15.5% efficiency. The number of PV panels are determined according to the shape and result of energy potential analysis of building roofs in ArcMap tool. On occasion of the incompatibility of some roofs with the selected PV size, some unavailable roof parts are excluded and consequently the number of the most available roof surface to install PV is determined as $13,320$ m^2 and the number of panels approximately 8,818 regarding to the selected photovoltaic panel.

5. CONCLUSION

To calculate solar radiation in a specific region, there are some various improved methods and models. Some of the models considers only meteorological parameters such as temperature, air pressure, sunshine duration hours to compute the possible amount of solar radiation. The other models take into account latitude, longitude and elevation which are geological characteristics. In this thesis, both methods depending atmospheric and topographical factors are incorporated. The purpose of this is to perform a reliable study and obtain accurate results for solar energy potential in Eskişehir.

This thesis divided into three main parts. In these parts, estimation, simulation and visual applications related with the solar radiation are implemented. The calculations highly depends on the monthly and hourly global solar radiation values. The models and methods are applied to a case study of Eskişehir. In ArcGIS, the solar radiation maps are generated in yearly and this study results are belonged to Engineering Faculty, İki Eylül Campus of Anadolu University, Eskişehir.

In the first part, six different models are used for calculations of total monthly solar radiation derived from hourly global solar radiation. Furthermore, the statistical error indication methods are used by virtue of selection of the model which has highest accuracy. As a result of the comparison of isotropic and an isotropic models, the Badescu model is favorable in solar radiation calculation on a tilted surface. All the results of statistical error indication methods points out the Badescu model had considerably high performance results and least error.

The second part composed of two different PV simulation algorithm. First one depends on MATLAB/Simulink and it is an ideal PV panel simulation. The ideal

PV panel simulation results show that the general characteristics of the PV module. After establishing the ideal PV simulation, the simulation of the PV module is implemented by taking advantage of the hourly global solar radiation estimation results and meteorological condition measurements. The simulation from estimated effective solar radiation results gives the possible PV panel power generation value. By virtue of the changes of the incoming solar radiation amount and the cell temperature, the possible generated power of a PV module has not same value and has a fluctuations throughout the year. Simulation results show that temperature plays a central role because of the reducing output with increasing cell temperature in power generation of a PV module.

In the third part of the study, the solar energy potential is determined on the Solar Analyst tool at ArcGIS using DSM data Engineering Faculty of Anadolu University İki Eylül Campus by considered some geological factors. The results show that azimuth factor has an important role on solar radiation, south facing parts of building roofs receive most amount of radiation and tilt angle is also identifier factor. The results verified that the annual solar potential on vertical rooftops is less than the smooth parts. The outcome of this study can assist decision makers or researchers to visualize building rooftop PV potential in specific surfaces, and further select suitable areas to install PV systems.

In this thesis, a comprehensive study is realized to obtain the accurate result related with the solar radiation for PV installation. Finally it is concluded that Badescu model is a reliable model and well capable to estimate solar energy for latitude based tilt angle in Eskişehir. There are two PV application model: ideal PV simulation and the PV simulation depending on Badescu model demonstrates

the possible generated power in hour. Purpose of constructing two PV simulation algorithms, to assess the efficiency of the PV panel in Eskişehir. Both two PV simulations supplies a view towards the effective factors of PV power generation such as temperature and wind. It can be understood that from the results of these simulations, temperature has an overwhelming effect compared to the wind speed and the pressure on power generation of PV array.

In response to the objective, the Engineering Faculty PV potential is calculated in two ways. By using PV array algorithm adjusted to the Badescu model and available building roof surface calculation result from ArcGIS study, the Engineering PV potential is calculated. The other PV potential calculation depends on ArcGIS Solar Analyst. Thus, it is important to interpret the results of the methods. The results of the two PV potential studies have some difference. Although ArcGIS study uses detailed surface information, it is not able to consider the some weather parameters. Similarly, Badescu model does not include a calculation regarding to building surface footprints.

Building roofs which can be used for collecting solar radiation. A raster based ArcGIS study not only gives an information of solar energy potential but also supplies a decision whether the building roofs are available for PV installation or not. Thanks to ArcGIS program, required number of PV panels are calculated and unavailable surfaces of building roofs are excluded. Consequently, the Engineering Faculty has a respectable amount of solar energy potential and 8,818 solar panel capacity.

In this case, there is not a unique solution to determine solar energy potential. When this thesis is compared to many other studies, it is more applicable and func-

tional because this study not only provides an information about the PV potential of the selected region but also gives an idea about the availability of the building roofs to PV installation. In addition, by means of PV simulations, possible PV losses can be observed for all the year. As a consequence, the methods presented and tested in this thesis can also be adjusted and generalized to other cities with intent to meet energy demand of selected places.

REFERENCES

[1] R. Mejdoul and M. Taqi. The mean hourly global radiation prediction models investigation in two different climate regions in morocco. *International Journal of Renewable Energy Research*, 2(4):608–617, 2012.

[2] C.A Gueymard and D.R. Myers. Validation and ranking methodologies for solar radiation models. In *Modeling solar radiation at the earth's surface*, pages 479–510. Springer, 2008.

[3] K.N. Poudyal, B.K. Bhattarai, B. Sapkota, and B. Kjeldstad. Estimation of global solar radiation using clearness index and cloud transmittance factor at trans-himalayan region in nepal. *Energy and power engineering*, 4(06):415, 2012.

[4] R. Yacef, A. Mellit, S. Belaid, and Z. Şen. New combined models for estimating daily global solar radiation from measured air temperature in semi-arid climates: application in ghardaïa, algeria. *Energy Conversion and Management*, 79:606–615, 2014.

[5] R.G. Allen. Self-calibrating method for estimating solar radiation from air temperature. *Journal of Hydrologic engineering*, 2(2):56–67, 1997.

[6] S. Janjai, P. Praditwong, and C. Moonin. A new model for computing monthly average daily diffuse radiation for bangkok. *Renewable Energy*, 9(1-4):1283–1286, 1996.

[7] J. Fan, X. Wang, L. Wu, F. Zhang, H. Bai, X. Lu, and Y. Xiang. New combined models for estimating daily global solar radiation based on sunshine duration in humid regions: A case study in south china. *Energy Conversion and Management*, 156:618–625, 2018.

[8] R. Li, L. Zhao, T. Wu, Y. Ding, Y. Xin, D. Zou, Y. Xiao, Y. Jiao, Y. Qin, and L. Sun. Temporal and spatial variations of global solar radiation over the qinghai–tibetan plateau during the past 40 years. *Theoretical and applied climatology*, 113(3-4):573–583, 2013.

[9] J. Almorox, C. Hontoria, and M. Benito. Models for obtaining daily global solar radiation with measured air temperature data in madrid (spain). *Applied Energy*, 88(5):1703–1709, 2011.

[10] M. Benghanem and A. Mellit. A simplified calibrated model for estimating daily global solar radiation in madinah, saudi arabia. *Theoretical and applied climatology*, 115(1-2):197–205, 2014.

[11] K.L. Bristow and G.S. Campbell. On the relationship between incoming solar radiation and daily maximum and minimum temperature. *Agricultural and forest meteorology*, 31(2):159–166, 1984.

[12] P.E. Thornton and S.W. Running. An improved algorithm for estimating incident daily solar radiation from measurements of temperature, humidity, and precipitation. *Agricultural and Forest Meteorology*, 93(4):211–228, 1999.

[13] T. Khatib, A. Mohamed, and K. Sopian. A review of solar energy modeling techniques. *Renewable and Sustainable Energy Reviews*, 16(5):2864–2869, 2012.

[14] C. Demain, M. Journée, and C. Bertrand. Evaluation of different models to estimate the global solar radiation on inclined surfaces. *Renewable Energy*, 50:710–721, 2013.

[15] M. J. Ahmad and G. N. Tiwari. Optimization of tilt angle for solar collector to receive maximum radiation. *The Open Renewable Energy Journal*, 2(1), 2009.

[16] H. Darhmaoui and D. Lahjouji. Latitude based model for tilt angle optimization

for solar collectors in the mediterranean region. *Energy Procedia*, 42:426–435, 2013.

[17] KN. Shukla, S. Rangnekar, and K. Sudhakar. Comparative study of isotropic and anisotropic sky models to estimate solar radiation incident on tilted surface: A case study for bhopal, india. *Energy Reports*, 1:96–103, 2015.

[18] F.A. Al-Sulaiman and B. Ismail. Estimation of monthly average daily and hourly solar radiation impinging on a sloped surface using the isotropic sky model for dhahran, saudi arabia. *Renewable Energy*, 11(2):257–262, 1997.

[19] S. Sandhya, R.N. Starbell, and G.J.J. Wessley. Modeling and analysis of latitude-based solar radiation models suitable for indian cities. *Journal of Basic and Applied Engineering Research*, 1(9):120–123, 2014.

[20] B. Liu and R. Jordan. Daily insolation on surfaces tilted towards equator. *ASHRAE J.;(United States)*, 10, 1961.

[21] P.S. Koronakis. On the choice of the angle of tilt for south facing solar collectors in the athens basin area. *Solar Energy*, 36(3):217–225, 1986.

[22] V. Badescu. 3d isotropic approximation for solar diffuse irradiance on tilted surfaces. *Renewable Energy*, 26(2):221–233, 2002.

[23] J.E. Hay. Calculation if the solar radiation incident on inclined surfaces. In *Proceedings first Canadian Solar Radiation Data Workshop, Toronto. Ontario, Canada 1978*, 1978.

[24] D.T. Reindl, W.A. Beckman, and J.A. Duffie. Evaluation of hourly tilted surface radiation models. *Solar energy*, 45(1):9–17, 1990.

[25] J.A. Duffie and W.A. Beckman. *Solar engineering of thermal processes*. John Wiley & Sons, 2013.

[26] A.Q. Jakhrani, S.R. Samo, A.R.H. Rigit, and S.A. Kamboh. Selection of models for calculation of incident solar radiation on tilted surfaces. *World Applied Sciences Journal*, 22(9):1334–1343, 2013.

[27] R. Mubarak, M. Hofmann, S. Riechelmann, and G. Seckmeyer. Comparison of modelled and measured tilted solar irradiance for photovoltaic applications. *Energies*, 10(11):1688, 2017.

[28] S.A.M. Maleki, H. Hizam, and C. Gomes. Estimation of hourly, daily and monthly global solar radiation on inclined surfaces: Models re-visited. *Energies*, 10(1):134, 2017.

[29] Y. El Mghouchi, T. Ajzoul, and A. El Bouardi. Prediction of daily solar radiation intensity by day of the year in twenty-four cities of morocco. *Renewable and Sustainable Energy Reviews*, 53:823–831, 2016.

[30] C.K. Pandey and A.K. Katiyar. A comparative study to estimate daily diffuse solar radiation over india. *Energy*, 34(11):1792–1796, 2009.

[31] P. Fu and P.M. Rich. Design and implementation of the solar analyst: an arcview extension for modeling solar radiation at landscape scales. In *Proceedings of the Nineteenth Annual ESRI User Conference*, volume 1, pages 1–31, 1999.

[32] J. Hofierka, M. Suri, et al. The solar radiation model for open source gis: implementation and applications. In *Proceedings of the Open source GIS-GRASS users conference*, volume 2002, pages 51–70, 2002.

[33] Y. Choi, J. Rayl, C. Tammineedi, and J.R.S Brownson. Pv analyst: Coupling arcgis with trnsys to assess distributed photovoltaic potential in urban areas. *Solar Energy*, 85(11):2924–2939, 2011.

[34] G. Agugiaro, F. Nex, F. Remondino, R. De Filippi, S. Droghetti, and

C. Furlanello. Solar radiation estimation on building roofs and web-based so-lar cadastre. *ISPRS Ann. Photogramm. Remote Sens. Spat. Inf. Sci*, 1:177–182, 2012.

[35] L. Bergamasco and P. Asinari. Scalable methodology for the photovoltaic solar energy potential assessment based on available roof surface area: Application to piedmont region (italy). *Solar Energy*, 85(5):1041–1055, 2011.

[36] L.K. Wiginton, H.T. Nguyen, and J.M. Pearce. Quantifying rooftop solar photo-voltaic potential for regional renewable energy policy. *Computers, Environment and Urban Systems*, 34(4):345–357, 2010.

[37] F. Borfecchia, E. Caiaffa, M. Pollino, L. De Cecco, S. Martini, L. La Porta, and A. Marucci. Remote sensing and gis in planning photovoltaic potential of urban areas. *European Journal of Remote Sensing*, 47(1):195–216, 2014.

[38] J. Esclapés, I. Ferreiro, J. Piera, and J. Teller. A method to evaluate the adapt-ability of photovoltaic energy on urban façades. *Solar Energy*, 105:414–427, 2014.

[39] J. Byrne, J. Taminiau, L. Kurdgelashvili, and K.N. Kim. A review of the so-lar city concept and methods to assess rooftop solar electric potential, with an illustrative application to the city of seoul. *Renewable and Sustainable Energy Reviews*, 41:830–844, 2015.

[40] J. Hofierka and M. Zlocha. A new 3-d solar radiation model for 3-d city models. *Transactions in GIS*, 16(5):681–690, 2012.

[41] C. Catita, J. Redweik, P.and Pereira, and M.C. Brito. Extending solar potential analysis in buildings to vertical facades. *Computers & Geosciences*, 66:1–12, 2014.

[42] K.K.L. Lau, F. Lindberg, E. Johansson, M.I. Rasmussen, and S. Thorsson. In-

vestigating solar energy potential in tropical urban environment: A case study of dar es salaam, tanzania. *Sustainable Cities and Society*, 30:118–127, 2017.

[43] H. Takebayashi, E.o Ishii, M. Moriyama, A. Sakaki, S. Nakajima, and H. Ueda. Study to examine the potential for solar energy utilization based on the relationship between urban morphology and solar radiation gain on building rooftops and wall surfaces. *Solar Energy*, 119:362–369, 2015.

[44] Y. Li, D. Ding, C. Liu, and C. Wang. A pixel-based approach to estimation of solar energy potential on building roofs. *Energy and Buildings*, 129:563–573, 2016.

[45] L. Cheng, H. Xu, S. Li, Y. Chen, F. Zhang, and M. Li. Use of lidar for calculating solar irradiance on roofs and façades of buildings at city scale: Methodology, validation, and analysis. *ISPRS Journal of Photogrammetry and Remote Sensing*, 138:12–29, 2018.

[46] K. Suomalainen, V. Wang, and B. Sharp. Rooftop solar potential based on lidar data: Bottom-up assessment at neighbourhood level. *Renewable Energy*, 111:463–475, 2017.

[47] A. Teke, H.B. Yıldırım, and Ö. Çelik. Evaluation and performance comparison of different models for the estimation of solar radiation. *Renewable and Sustainable Energy Reviews*, 50:1097–1107, 2015.

[48] Z. Jin, W. Yezheng, and Y. Gang. General formula for estimation of monthly average daily global solar radiation in china. *Energy Conversion and Management*, 46(2):257–268, 2005.

[49] A. Marzo, M. Trigo-Gonzalez, J. Alonso-Montesinos, M Martínez-Durbán, G López, P. Ferrada, E. Fuentealba, M. Cortés, and F.J. Batlles. Daily global

solar radiation estimation in desert areas using daily extreme temperatures and extraterrestrial radiation. *Renewable Energy*, 113:303–311, 2017.

[50] A. Mellit and A.M. Pavan. A 24-h forecast of solar irradiance using artificial neural network: Application for performance prediction of a grid-connected pv plant at trieste, italy. *Solar Energy*, 84(5):807–821, 2010.

[51] V.H. Quej, J. Almorox, J. A. Arnaldo, and L. Saito. Anfis, svm and ann soft-computing techniques to estimate daily global solar radiation in a warm sub-humid environment. *Journal of Atmospheric and Solar-Terrestrial Physics*, 155:62–70, 2017.

[52] A. Gani, K. Mohammadi, S. Shamshirband, H. Khorasanizadeh, J. Danesh, A.S.and Piri, Z. Ismail, and M. Zamani. Day of the year-based prediction of horizontal global solar radiation by a neural network auto-regressive model. *Theoretical and applied climatology*, 125(3-4):679–689, 2016.

[53] K. Mohammadi, S. Shamshirband, C.W. Tong, K. A. Alam, and D. Petković. Potential of adaptive neuro-fuzzy system for prediction of daily global solar radiation by day of the year. *Energy Conversion and Management*, 93:406–413, 2015.

[54] A. S. Sedra and K. C. Smith. Microelectronic circuits. london, u.k. *Journal of Physics: Conference Series*, 710:012032, 2006.

[55] H.J. Möller. Semiconductors for solar cells. norwood, ma: Artech house, 1993.

[56] A.L. Fahrenbruch and R.H. Bube. Fundamentals of solar cells (academic, san francisco, ca, 1983). *Google Scholar*.

[57] D. Dondi, D. Brunelli, L. Benini, P. Pavan, A. Bertacchini, and L. Larcher. Photovoltaic cell modeling for solar energy powered sensor networks. In *Advances*

in Sensors and Interface, 2007. IWASI 2007. 2nd International Workshop on, pages 1–6. IEEE, 2007.

[58] H. Patel and V. Agarwal. Matlab-based modeling to study the effects of partial shading on pv array characteristics. *IEEE transactions on energy conversion*, 23(1):302–310, 2008.

[59] J.A. Gow and C.D. Manning. Development of a photovoltaic array model for use in power-electronics simulation studies. *IEE Proceedings-Electric Power Applications*, 146(2):193–200, 1999.

[60] N Pongratananukul and T Kasparis. Tool for automated simulation of solar arrays using general-purpose simulators. In *Computers in Power Electronics, 2004. Proceedings. 2004 IEEE Workshop on*, pages 10–14. IEEE, 2004.

[61] K. Ishaque, Z. Salam, and H. Taheri. Simple, fast and accurate two-diode model for photovoltaic modules. *Solar energy materials and solar cells*, 95(2):586–594, 2011.

[62] K. Nishioka, N. Sakitani, Y. Uraoka, and T. Fuyuki. Analysis of multicrystalline silicon solar cells by modified 3-diode equivalent circuit model taking leakage current through periphery into consideration. *Solar Energy Materials and Solar Cells*, 91(13):1222–1227, 2007.

[63] S. Chowdhury, GA. Taylor, SP. Chowdhury, AK Saha, and YH Song. Modelling, simulation and performance analysis of a pv array in an embedded environment. In *Universities Power Engineering Conference, 2007. UPEC 2007. 42nd International*, pages 781–785. IEEE, 2007.

[64] I.H. Altas and A.M. Sharaf. A photovoltaic array simulation model for matlab-simulink gui environment. In *Clean Electrical Power, 2007. ICCEP'07. Interna-*

tional Conference on, pages 341–345. IEEE, 2007.

[65] J.A. Kratochvil, W.E. Boyson, and D.L. King. Photovoltaic array performance model. Technical report, Sandia National Laboratories, 2004.

[66] P. Talebizadeh, MA. Mehrabian, and M. Abdolzadeh. Prediction of the optimum slope and surface azimuth angles using the genetic algorithm. *Energy and buildings*, 43(11):2998–3005, 2011.

[67] M. Iqbal. *An introduction to solar radiation*. Elsevier, 2012.

[68] D.G. Erbs, S.A. Klein, and J.A. Duffie. Estimation of the diffuse radiation fraction for hourly, daily and monthly-average global radiation. *Solar energy*, 28(4):293–302, 1982.

[69] M.M. de Oliveira Junior, R.N.N. Koury, L. Machado, and A. Maia. Development of software to estimate the solar radiation on fixed sloped surfaces. 2013.

[70] A.Q. Jakhrani, A.K. Othman, AR. Rigit, S.R. Samo, and S. Kamboh. Estimation of incident solar radiation on tilted surface by different empirical models. *International Journal of Scientific and Research Publications*, 2(12):1–6, 2012.

[71] C. Breyer and J. Schmid. Global distribution of optimal tilt angles for fixed tilted pv systems. *horizon*, 4444444(2):1, 2010.

[72] A.M. Haque, S. Sharma, and D. Nagal. Simulation of photovoltaic array using matlab/simulink: Analysis, comparison & results. *Futuristic Trends in Engineering, Science, Humanities, and Technology FTESHT-16*, page 60, 2016.

[73] M.G. Villalva, J.R. Gazoli, and E. R.Filho. Modeling and circuit-based simulation of photovoltaic arrays. In *Power Electronics Conference, 2009. COBEP'09. Brazilian*, pages 1244–1254. IEEE, 2009.

[74] W. De Soto, SA. Klein, and WA. Beckman. Improvement and validation of a

model for photovoltaic array performance. *Solar energy*, 80(1):78–88, 2006.

[75] V. Badescu. *Modeling solar radiation at the earth's surface*. Springer, 2014.

[76] B. Kroposki, W. Marion, D.L King, W.E. Boyson, and JA. Kratochvil. Comparison of module performance characterization methods. In *Photovoltaic Specialists Conference, 2000. Conference Record of the Twenty-Eighth IEEE*, pages 1407–1411. IEEE, 2000.

[77] A.H. Fanney, M.W. Davis, and B.P. Dougherty. Short-term characterization of building integrated photovoltaic panels. In *ASME Solar 2002: International Solar Energy Conference*, pages 211–221. American Society of Mechanical Engineers, 2002.

[78] O. Gil-Arias and E.I. Ortiz-Rivera. A general purpose tool for simulating the behavior of pv solar cells, modules and arrays. In *Control and Modeling for Power Electronics, 2008. COMPEL 2008. 11th Workshop on*, pages 1–5. IEEE, 2008.

[79] K. Bitirgen and Ü. Başaran Filik. Solar electricity potential based on arcgis maps and consumption of energy for engineering faculty buildings in anadolu university. In *Electrical and Electronics Engineering (ELECO), 2017 10th International Conference on*, pages 156–160. IEEE, 2017.

[80] X. Huang. A future energy harvesting scenario for georgia tech campus using photovoltaic solar panels and piezoelectric materials. 2016.

[81] R. Margolis, P. Gagnon, J. Melius, C. Phillips, and R. Elmore. Using gis-based methods and lidar data to estimate rooftop solar technical potential in us cities. *Environmental Research Letters*, 12(7):074013, 2017.

[82] F.M. Markos and J Sentian. Potential of solar energy in kota kinabalu, sabah:

An estimate using a photovoltaic system model. *Journal of Physics: Conference Series*, 710:012032, 2016.

[83] H. Duzen and H. Aydin. Sunshine-based estimation of global solar radiation on horizontal surface at lake van region (turkey). *Energy Conversion and Management*, 58:35–46, 2012.

[84] K.A. Moharram, MS. Abd-Elhady, HA. Kandil, and H. El-Sherif. Enhancing the performance of photovoltaic panels by water cooling. *Ain Shams Engineering Journal*, 4(4):869–877, 2013.

[85] H. Bahaidarah, A. Subhan, P. Gandhidasan, and S. Rehman. Performance evaluation of a pv (photovoltaic) module by back surface water cooling for hot climatic conditions. *Energy*, 59:445–453, 2013.

[86] http://abcsolar.com/pdf/schott165.pdf. (Date of access: 10.05.2018).

CURRICULUM VITAE

Name Surname   : Kübra BİTİRGEN..

Language   : English, İtalian..

Birth Place and Date : Eskişehir/1992..

Email Adress   : kubra92eski@gmail.com....................................

Educational:

- 2016-2018 : Anadolu University (Graduate) Electrical and Electronics Engineering Department GPA: 3.60/ 4.00

- 2016   : Labor safety officer document

- 2011-2016 : Anadolu University University (Undergraduate) Electrical and Electronics Engineering Department GPA: 3.05 / 4.00

Publications and Scientific or Artistic Activities:

- Bitirgen, K. (2017), 2017, IEEE, Solar electricity potential based on ArcGIS maps and consumption of energy for engineering faculty buildings in Anadolu University, 2017 10th International Conference on, 156–160.

Fields of Interest:

- Power systems, Solar energy, Electrical circuit simulations.